Studies of new inorganic species using relativistic quantum chemistry

Dissertation for the degree of Doctor Philosophiae

Michael Patzschke

University of Helsinki
Department of Chemistry
Laboratory for Instruction in Swedish
P.O. Box 55 (A.I. Virtasen Aukio 1)
FIN-00014 University of Helsinki, Finland

To be presented, with permission of the Faculty of Science, University of Helsinki, for public discussion in Auditorium A129, Department of Chemistry (A.I. Virtasen Aukio 1, Helsinki), June the 27th, 2006.

Helsinki 2006

Supervised by

Prof. Pekka Pyykkö
Department of Chemistry
University of Helsinki

Reviewed by

Prof. Matti Hotokka
Department of Chemistry
Åbo Akademi

Prof. Trond Saue
Department of Chemistry
University of Strasbourg

ISBN 952-92-0519-8 (paperback)
ISBN 952-10-3229-4 (PDF)
http://ethesis.helsinki.fi

Yliopistopaino Helsinki 2006

Parsifal: *Ich schreite kaum, doch wähn' ich mich schon weit.*
Gurnemanz: *Du siehst, mein Sohn, zum Raum wird hier die Zeit.*

"Parsifal" 1st act, by Richard Wagner (1877)

Abstract

In the present work the methods of relativistic quantum chemistry have been applied to a number of small systems containing heavy elements, for which relativistic effects are important. First, a thorough introduction of the methods used is presented. This includes some of the general methods of computational chemistry and a special section dealing with how to include the effects of relativity in quantum chemical calculations.

Second, after this introduction the results obtained are presented. Investigations on high-valent mercury compounds are presented and new ways to synthesise such compounds are proposed.

The methods described were applied to certain systems containing short Pt-Tl contacts. It was possible to explain the interesting bonding situation in these compounds.

One of the most common actinide compounds, uranium hexafluoride was investigated and a new picture of the bonding was presented. Furthermore the rareness of uranium-cyanide compounds was discussed.

In a foray into the chemistry of gold, well known for its strong relativistic effects, investigations on different gold systems were performed. Analogies between Au^+ and platinum on one hand and oxygen on the other were found. New systems with multiple bonds to gold were proposed to experimentalists. One of the proposed systems was spectroscopically observed shortly afterwards. A very interesting molecule, which was theoretically predicted a few years ago is WAu_{12}. Some of its properties were calculated and the bonding situation was discussed. In a further study on gold compounds it was possible to explain the substitution pattern in bis[phosphane-gold(I)] thiocyanate complexes. This is of some help to experimentalists as the systems could not be crystallised and the structure was therefore unknown.

Finally, computations on one of the heaviest elements in the periodic table were performed. Calculation on compounds containing element 110, darmstadtium, showed that it behaves similarly as its lighter homologue platinum. The extreme importance of relativistic effects for these systems was also shown.

List of Publications

List of publications included in the thesis

I. Pyykkö, P.; Straka, M.; Patzschke, M. "HgH_4 and HgH_6: further candidates for high-valent mercury compounds", *Chem.Comm.* **2002**, 1728

II. Pyykkö, P.; Patzschke, M. "On the nature of the short Pt-Tl bonds in model compounds $[H_5Pt\text{-}TlH_n]^{n-}$", *Faraday Discuss.* **2003**, *124*, 41

III. Straka, M.; Patzschke, M.; Pyykkö, P. "Why are uranium cyanides rare while U-F and U-O bonds are common and short", *Theor.Chem.Acc.* **2003**, *109*, 332

IV. Autschbach, J.; Hess, B. A.; Johansson, M. P.; Neugebauer, J.; Patzschke, M.; Pyykkö, P.; Reiher, M.; Sundholm, D. "Properties of WAu_{12}", *Phys.Chem.Chem.Phys.* **2004**, *6*, 11

V. Pyykkö, P.; Patzschke, M.; Suurpere, J. "Calculated structures of $[Au{=}C{=}Au]^{2+}$ and related systems", *Chem.Phys.Lett.* **2003**, *381*, 45

VI. Berger, R. J. F.; Patzschke, M.; Sundholm, D.; Schneider, D.; Schmidbaur, H. "Isomeric Mono- and Bis[phosphane-gold(I)] Thiocyanate Complexes", *Chem.Eur.J.* **2005**, *11*, 3574

VII. Patzschke, M.; Pyykkö, P. "Darmstadtium carbonyl and carbide resemble platinum carbonyl and carbide", *Chem.Comm.* **2004**, 1982

List of other publications

I. Juselius, J.; Patzschke, M.; Sundholm, D. "Calculation of ring-current susceptibilities for homo-aromatic molecules", *J.Mol.Struct.(Theochem)* **2003**, *633*, 123

II. Henriksson, K. O. E.; Nordlund, K.; Keinonen, J.; Sundholm, D.; Patzschke, M. "Simulations of the initial stages of blistering in helium implanted tungsten", *Physica Scripta* **2004**, *T108*, 95

III. Patzschke, M.; Sundholm, D. "Density-Functional-Theory Studies of the Infrared Spectra of Titanium-Carbide Nanocrystals", *J.Phys.Chem.B* **2005**, *109*, 12503

IV. Pyykkö, P.; Riedel, S.; Patzschke, M. "Triple-Bond Covalent Radii", *Chem.Eur.J.* **2005**, *11*, 3511

V. Patzschke, M.; Jensen, H. J. Aa.; Pedersen, J. K.; Pyykkö, P. "On the colour of Bi(V) compounds, a relativistic study", to be submitted

Acknowledgments

The research for this work was conducted at the University of Helsinki from September 2001 to March 2005. This work would not have been possible without the help of numerous people. First of all I owe my gratitude to my supervisor Pekka Pyykkö. He is not only an outstanding scientist, he was also a very good supervisor. His physical understanding and chemical intuition paired with an enormous knowledge of the scientific literature was very helpful and never ceased to amaze me.

I am happy, that I had the opportunity to work with Henrik Konschin and Dage Sundholm. I learned a lot from them. During my whole stay in Helsinki they were more than supportive. I very much enjoyed the discussions with my colleagues Jonas Juselius, Michal Straka and Tommy Vänskä on all kinds of subjects. These were not only funny, but also thought-provoking and inspiring. My special thanks go to our secretary Susanne Lundberg. She was always helpful and her cheerful manners brightened the days.

I am very grateful for all the help, support and encouragement I got from the rest of the people at the Laboratory for Instruction in Swedish. I have never worked in a more friendly and more inspiring atmosphere. For me it was especially gratifying, that I was allowed to teach young students. Meeting them and kindling their interest in chemistry is a unique experience.

Scientific work benefits from discussion and collaboration. My research would not have been as interesting and gratifying without my coworkers and the many people I met on conferences and schools. Especially I would like to thank Trygve Helgaker, Hans Jørgen Aagaard Jensen, Jeppe Olsen, Jesper Pedersen, Juha Vaara and Lucas Visscher. The reviewers of this thesis, Matti Hotokka and Trond Saue gave very helpful comments, I thank them for the effort they put into reviewing the manuscript. I would also like to thank Nik Kaltsoyannis for agreeing to be the opponent for this thesis.

A very special thank you to my dear friends Raphael Berger, Mikael Johansson and Pekka Manninen. I thank you for your friendship, for your support and for hours of interesting scientific and not so scientific discussions.

I want to express my gratitutde to my university teacher Dietrich Haase. He kindled my interest in theoretical chemistry. I will always be thankful for the enormous work he put into lecturing.

I would like to thank the Magnus Ehrnrooth Stiftelse, the MOLPROP network and the Academy of Finland for financial support. Computational resources were provided by the Finnish Centre for Scientific Computing (CSC). I also want to thank Nino Runeberg from CSC for always providing fast and professional help.

Besides my scientific interests I very much enjoy music. I would like to thank the members of the Chorus Sanctæ Ceciliæ for the many hours of singing we enjoyed together. Especially Dag-Ulrik Almqvist and Aasa Feragen made my stay in Helsinki a happy one.

A thank you to my parents and all my friends in Germany and elsewhere in the world. You all have helped me in various ways during the last few years. There are too many to fit all the names on one page, but you know who you are and you have my gratitude.

Finally, what is life without love? Ansku, you were the one who brought back love into my life. You helped me more than I can ever express in words. This thesis would not have been written without your support. Thank you for everything!

Helsinki, May 2006 Michael Patzschke

Contents

List of Abbreviations

ADC	Algebraic Diagrammatic Construction
ANO	Atomic Natural Orbital
AO	Atomic Orbital
BSSE	Basis-Set Superposition Error
CASSCF	Complete Active Space SCF
CASPT2	CASSCF with added Perturbation Theory to 2nd order
CC	Coupled Cluster
CCSD	Coupled Cluster with Single and Double excitations
CGTO	Contracted GTO
CI	Configuration Interaction
CISD	Configuration Interaction with Single and Double excitations
CPHF	Coupled Perturbed Hartree-Fock
CSF	Configuration State Function
DFT	Density Functional Theory
ECP	Effective Core Potential
ELF	Electron-Localisation Function
ESC	Elimination of the Small Component
FCI	Full CI
GGA	Generalised Gradient Approximation
GTO	Gaussian-Type Orbital
HF	Hartree-Fock
HOMO	Highest Occupied MO
LCAO-MO	Linear Combination of Atomic Orbitals to form Molecular Orbitals
L(S)DA	Local (Spin) Density Approximation
LUMO	Lowest Unoccupied MO
MCSCF	Multi Configuration SCF
MPn	Møller-Plesset perturbation theory to the nth order
MO	Molecular Orbital
PGTO	Primitive GTO
QCISD	Quadratic Configuration Interaction with Single and Double excitations
QED	Quantum Electro Dynamics
RI	Resolution of the Identity
RPA	Random Phase Approximation
SCF	Self-Consistent Field
SIC	Sef-Interaction Corrected
STO	Slater-Type Orbital
(S)VWN	L(S)DA functional developed by Vosko, Wilk and Nusair
ZORA	Zeroth Order Regular Approximation

Chapter 1

Introduction

Relativistic quantum chemistry is one of the most interesting areas of chemistry. In it, two of the most important physical theories of the last century are united. The quantum theory, which revolutionised our understanding of very small systems (such as atoms and molecules) and the theory of relativity, which brought new understanding of very large systems (like galaxies). Only the combination of these two theories makes it possible to understand the properties of certain elements and their compounds.

The importance of relativity in the field of chemistry was even disputed by one of the fathers of relativistic quantum mechanics, P.A.M. Dirac. However, it was soon understood, that a relativistic treatment was necessary for heavy elements. The inner electrons of heavy elements move very fast, this leads to a relativistic shrinkage of the 1s orbitals. This effect is transferred to the other orbitals of same angular momentum l. The s orbitals are relativistically contracted. Another relativistic effect is spin-orbit coupling which leads to the splitting of shells with $l > 0$ into the two $l \pm 1/2$ subshells. The $p_{1/2}$ shell is also contracted, the effect on the $p_{3/2}$ shell is rather small. The contracted s and p orbitals shield the nucleus better and therefore orbitals of higher angular momentum will be radially enlarged. These three effects can be seen in Figure 1.1 for the outermost orbitals of Cm^{3+}.

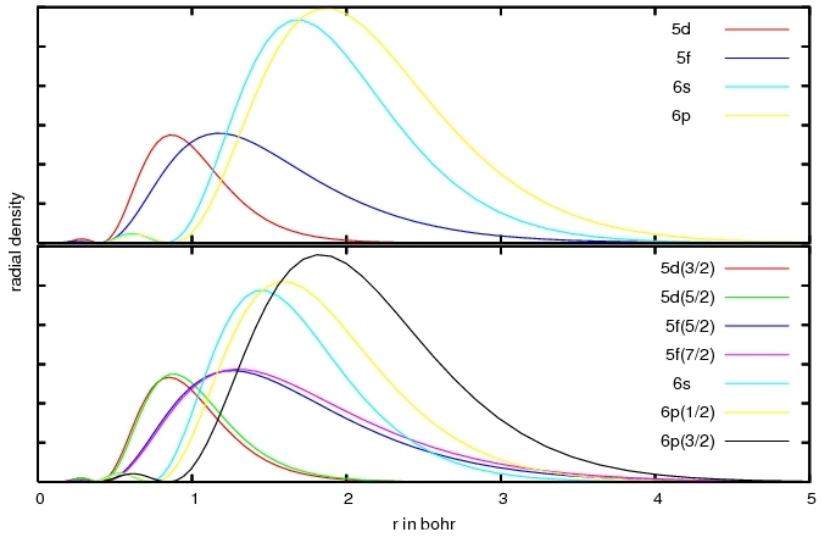

Figure 1.1: Comparison between the radial density of the outermost orbitals of Cm^{3+} calculated non-relativistically (top) and relativistically (bottom).

Relativistic effects influence the chemical behaviour of heavy elements.[1] The number of papers in the field has been growing rapidly. A very good survey of the available literature can be found in 2, 3, 4 and 5. Some well-known effects are the low melting point of mercury and the fact that the lead accumulator actually works. Probably the most widely known relativistic effect is the colour of gold.

In fact, the scalar relativistic effects show a pronounced maximum for gold.

The main interest in this thesis lay in systems where relativistic effects become important. Consequently we investigated a number of chemical compounds containing gold. Also the neighbours of gold in the periodic table, platinum and mercury, show pronounced relativistic effects. Compounds of these elements were therefore also studied. After the maximum of relativistic effects for gold one has to go the the actinides to get relativistic effects of the same magnitude. One of the most common actinides, for which a lot of experimental data can be found, is uranium. We consequently studied various uranium compounds. For the even heavier transactinides relativistic effects are of course extremely important. A study of compounds of the transactinide darmstadtium concludes this thesis.

Although relativistic quantum chemistry is not a very new field, there are still many experimental observations that need to be explained. The cooperation of theoreticians and experimentalists is needed to fully understand the chemistry of systems containing heavy elements. The thesis was written in the hope to aid this cooperation.

Chapter 2

Theoretical Foundations

In the following the methods used for the research carried out will be described in some detail. It is very important to have a solid understanding of the methods one wants to use, in order to be aware of their shortcomings and advantages. For a more in-depth review of theoretical methods, a number of textbooks is available.[6,7,8,9,10,11,12,13]

2.1 The Quantum Chemical Space

The goal of computational chemistry is to solve an eigenvalue equation of the following form

$$\hat{H}\Psi = \mathrm{E}\Psi \tag{2.1}$$

This is a formidable equation to solve even if it might not look like it in this simple form. The operator $\hat{H}$ can take different forms and in the simplest non-relativistic approximation the resulting equation is known as the Schrödinger equation.

As exact solutions for these equations are only possible for one-electron systems we have to use approximations. Basis sets are used to describe the electrons. Electron-electron interactions are modeled by different methods. Finally, different Hamiltonians can be used to describe the physics of the system at hand.

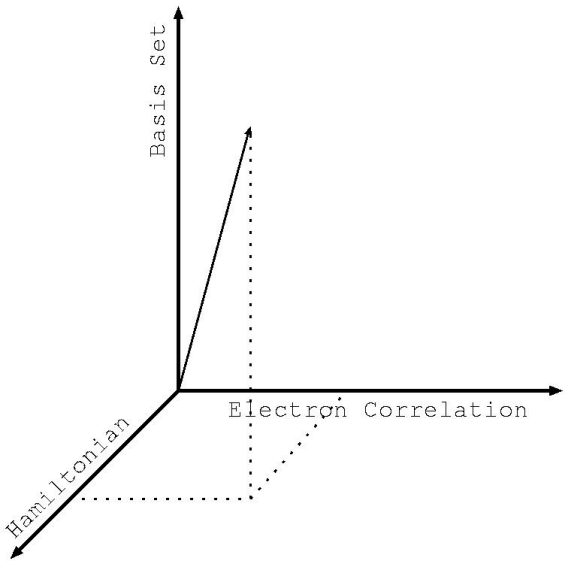

Figure 2.1: The space of accuracy of quantum chemical calculations.

The Figure 2.1 summarises how the accuracy of quantum chemical calculations can be influenced. Let the level of electron correlation be the x-axis, the size of the used basis set is shown on the y-axis and the accuracy of the used Hamiltonian is given on the z-axis. The computational cost of a calculation can then be expressed as:

$$\text{cost} \sim zy^x \tag{2.2}$$

Normally one would like to go as far as possible on all three axes in order to get the highest accuracy. This is impossible because the computational cost would be prohibitive. In the next three sections we will inspect the meaning of x, y and z-axis in more detail. But one thing should be noted at the beginning. It is not advantageous to go far on one axis and use only low accuracy on the other two. For example, it is not very wise to do huge 4-component calculations at the Hartree-Fock level with small basis sets. Unfortunately there is quite a number of such calculations published in the literature.

2.2 Electron Correlation

We shall begin our exploration of Figure 2.1 with the x-axis, with the level of electron correlation. For that we will first review the most basic method of quantum chemical calculations, the Hartree Fock method. It will become apparent why we then need to proceed to include electron correlation.

2.2.1 The Hartree-Fock Method

The starting point is the Schrödinger equation. For a many-electron system with point-like nuclei and no external potential this equation reads:

$$\hat{H} = -\frac{\hbar^2}{2}\sum_\alpha \frac{1}{m_\alpha}\nabla_\alpha^2 - \frac{\hbar^2}{2m_e}\sum_i \nabla_i^2 + \sum_\alpha \sum_{\beta>\alpha} \frac{Z_\alpha Z_\beta e^2}{r_{\alpha\beta}} - \sum_\alpha \sum_i \frac{Z_\alpha e^2}{r_{i\alpha}} + \sum_j \sum_{i>j} \frac{e^2}{r_{ij}} \tag{2.3}$$

Here i and j refer to the electrons while α and β refer to the nuclei. This equation depends on the position of the electrons and the nuclei. As the nuclei are much heavier than the electrons, they move much slower. It turns out to be an excellent approximation to consider the nuclei fixed. This is known as the Born-Oppenheimer approximation.[14] When this approximation is used, the first term in the equation above (the kinetic energy of the nuclei) disappears. The third term, the attraction between the nuclei and the electrons transforms into a static external potential created by the nuclei. With this we can rewrite the equation as:

$$\hat{H} = \sum_i \hat{h}_i + \sum_j \sum_{i>j} \frac{e^2}{r_{ij}} \tag{2.4}$$

The Schrödinger equation can be seen as a sum of one-particle Hamiltonians to which is added the sum of the Coulombic repulsion of the electrons. This last term which mixes electrons makes it impossible to separate the Schrödinger equation. As a zeroth order approximation, we can still use a product ansatz for the wavefunction. Omitting the electron spin it can be written as:

$$\Phi_0 = f_1(r_1, \theta_1, \phi_1) f_2(r_2, \theta_2, \phi_2) \cdots f_n(r_n, \theta_n, \phi_n) \tag{2.5}$$

This approximation is also known as the one-particle picture. The errors created by this approximation can be treated with different methods that describe the electron correlation.

The functions f have to be determined variationally be minimising the energy expression:

$$\frac{\int \Phi_0^* \hat{H} \Phi_0 dv}{\int \Phi_0^* \Phi_0 dv} \tag{2.6}$$

Minimising this expression is also known as the Hartree method.[15]

Pauli showed that a proper wavefunction for a system of independent fermion particles, i.e. electrons, should be antisymmetric with respect to the exchange of two electrons.[16] In the form presented above the Hartree method does not include spin. It is possible to add electron spin in this method. Even then an obvious disadvantage of the Hartree method is, that the wavefunction does not exhibit the required antisymmetric behaviour.

If one constructs a square-matrix of spin-orbitals which have the same electron along a given row and the same spin orbital in a given column, the determinant of this matrix has the required property of antisymmetry. This observation was made in 1929 by Slater and the determinant is also known as a Slater determinant.[17]

Using Slater determinants in the Hartree method leads to the Hartree-Fock (HF) method.[18,19] It is normally used self-consistently. That means, that a starting guess is used to describe the electrons. The initial orbitals can be obtained using a cheap method like an extended Hückel calculation. From this calculation, the field in which the electrons move can be described. Then one can solve the one-particle equation to get a better description of the electron. This procedure is repeated for all electrons until the resulting wavefunction and the total energy remain constant. This is known as the self consistent field (SCF) approach.

The one electron equations are of the form:

$$\hat{F}(1)\phi_i(1) = \epsilon_i\phi_i(1) \tag{2.7}$$

The Fock operator $\hat{F}$ in atomic units can be written as:

$$\hat{F}(1) \equiv \hat{h}(1) + \sum_{j=1}^{n/2}[2\hat{J}_j(1) - \hat{K}_j(1)] \tag{2.8}$$

with:

$$\hat{h}(1) \equiv -\frac{1}{2}\nabla_1^2 - \sum_\alpha \frac{Z_\alpha}{r_{1\alpha}} \tag{2.9}$$

$$\hat{J}_l(1)f(1) \equiv \int \frac{\phi_j^*(2)\phi_j(2)}{r_1 2} dv_2 f(1) \tag{2.10}$$

$$\hat{K}_l(1)f(1) \equiv \int \frac{\phi_j^*(2)f(2)}{r_1 2} dv_2 \phi_j(1) \tag{2.11}$$

In the equations above $\hat{J}_j$ is the Coulomb operator and $\hat{K}_j$ the exchange operator. The integration is over all space and f is some arbitrary function.

For all the approximations it employs, the Hartree-Fock method is surprisingly accurate. It recovers about 99% of the total energy of the system. The missing one percent is known as the correlation energy. As pointed out earlier, the HF method averages the interaction of an electron with the rest of the electrons. In reality, there should be a sharp decrease in the probability of finding one electron close to another one, the so called electron cusp. The change in the energy and the wavefunction associated with accounting for the correlated movement of the electrons is known as dynamic correlation. There is another form of correlation energy, the so called static correlation. There are systems, that cannot be described with a single Slater determinant, e.g. systems with partly filled subshells. To describe such multi-reference systems accurately a number of Slater determinants has to be used. Methods for this will be described later. These methods also recover the static correlation.

2.2.2 Perturbation Methods

As stated above, the Hartree-Fock method recovers most of the energy of a system. The missing correlation energy is only a small part. Consequently, we can assume, that this correlation can be treated as a perturbation of the Hartree-Fock system. Given the unperturbed Hamiltonian $\hat{H}^0$ we introduce a perturbation $\hat{H}'$ that will transform the unperturbed Hamiltonian into the real Hamiltonian

$\hat{H}$. We then have to relate the eigenvalues and eigenfunctions of the unperturbed system to those of the real system.

Introducing a parameter λ that can go from zero (the unperturbed system) to one (the fully perturbed system) we get:

$$\hat{H} = \hat{H}_0 + \lambda \hat{H}' \tag{2.12}$$

This leads to the following Schrödinger equation for the real system:

$$\hat{H}\psi_n = (\hat{H}^0 + \lambda \hat{H}')\psi_n = E_n \psi_n \tag{2.13}$$

As the real Hamiltonian depends on λ, both the wavefunction and the energy of the real system can be expressed as functions of λ. We can now expand both E_n and ψ_n as a Taylor series in powers of λ.

$$E_n = E_n^{(0)} + \lambda E_n^{(1)} + \lambda^2 E_n^{(2)} + \dots \tag{2.14}$$
$$\psi_n = \psi_n^{(0)} + \lambda \psi_n^{(1)} + \lambda^2 \psi_n^{(2)} + \dots \tag{2.15}$$

These expressions for E_n and ψ_n can now be used in the Schrödinger equation for the real system. This leads to a rather lengthy expression in which like powers of λ can be collected. Using this method we can in principle get any order of correction to $E_n^{(0)}$ and $\psi_n^{(0)}$ of the unperturbed system. This general form of perturbation theory is widely used in physics and is known as Rayleigh-Schrödinger perturbation theory.

In 1934 Møller and Plesset used this technique for atoms and molecules.[20] In their approach, also called, Møller-Plesset perturbation theory (MP) the unperturbed wavefunction is the Hartree-Fock wavefunction. The perturbation is thus the difference between the averaged electron interaction of the Hartree-Fock method and the true electrostatic repulsion of the electrons. This is also known as the fluctuation potential. The unperturbed Hamilton operator can be expressed as the sum of one-electron Fock operators from Equation (2.8). The resulting unperturbed Schrödinger equation is:

$$\hat{H}^0 \Phi_0 = \left(\sum_{l=1}^{n} \epsilon_l \right) \Phi_0 \tag{2.16}$$

Using MP theory, the Hartree-Fock energy can be written as:

$$E_{HF} = \langle \Phi_0 | \hat{H} | \Phi_0 \rangle = \langle \Phi_0 | \hat{H}^0 + \hat{H}' | \Phi_0 \rangle = \langle \psi_0^{(0)} | \hat{H}^0 | \psi_0^{(0)} \rangle + \langle \Phi_0 | \hat{H}' | \Phi_0 \rangle = E_0^0 + E_0^1 \tag{2.17}$$

This means, that the Hartree-Fock energy already includes first order corrections to the unperturbed system. Hence, in order to get a real improvement of the energy, one has to go at least to second order. The expression for the second-order energy correction reads:

$$E_0^{(2)} = \sum_{s \neq 0} \frac{|\langle \psi_s^{(0)} | \hat{H}' | \Phi^{(0)} \rangle|^2}{E_0^{(0)} - E_s^{(0)}} \tag{2.18}$$

where the summation runs over all but the ground state. It would be a formidable task to do this summation. As $\hat{H}'$ only contains two-electron terms, the only contributing parts of this sum come from double excitations. This simplifies the equation above to:

$$E_0^{(2)} = \sum_{a=n+1}^{\infty} \sum_{b=a+1}^{\infty} \sum_{i=j+1}^{n} \sum_{j=1}^{n-1} \frac{|\langle ab | r_{12}^{-1} | ij \rangle \langle ab | r_{12}^{-1} | ji \rangle|^2}{\epsilon_i + \epsilon_j - \epsilon_a - \epsilon_b} \tag{2.19}$$

The four sums include all possible double excitations from the ground-state Slater determinant. Calculating the second order energy correction in this way is called an MP2 calculation. It is often useful to reduce the computational effort, by not using all possible excitations, but only those of the

valence orbitals. The core orbitals will have a major contribution to the MP2 energy, but it will not change much in a chemical reaction.

Formulas for higher order MPn calculations have been derived and implemented. Olsen et al. have developed a method to calculate arbitrary order MPn energies from the full CI wavefunction.[21] This is of course not an economic way to do MPn calculations, but it showed two interesting features. The MPn series exhibits a sawtooth behaviour between even and odd members of the series. The even member being closer to the full CI energy then the next higher odd term. More importantly, simple systems, like Ne, HF or H_2O, have been found for which the MPn series does actually diverge.[22]

MP2 calculations have become an extremely useful tool for computational chemists. Due to a fortuitous error cancellation, it is usually quite close to the full CI energy. MP2 can describe dispersion interaction between molecular fragments and can therefore be used in systems where van der Waals interactions are important. From the second-order correction to the wave function, one can get MP2 natural-orbital occupation numbers. These give a good hint, if the system under observation is a multi configuration system. If the occupation numbers of virtual orbitals are high, say above 0.1, then a multi configuration treatment is called for. The orbitals that should be used in such a treatment are the occupied ones with a low occupation number (e.g. below 1.9) and the virtual ones with occupation numbers above 0.1. This is only a rough guideline. Chemical intuition, which is one of the most important tools of a computational chemist, should be used to check the selection.

2.2.3 Coupled Cluster Methods

A more generalised approach is the coupled cluster (CC) ansatz. It can be written as:

$$\Psi_0 = e^{\hat{T}}\Phi_0 \tag{2.20}$$

Where $\hat{T} = \hat{T}_1 + \hat{T}_2 + \hat{T}_3 + \ldots$ is the cluster operator which operates on the normalised ground-state Hartree-Fock wavefunction. The cluster operator is a sum of n-particle excitation operators $\hat{T}_n$. These can be expressed as:

$$\hat{T}_n = \sum_{ai \geq bj \geq ck \ldots} t_{abc\ldots}^{ijk\ldots} \hat{\tau}_{ijk\ldots}^{abc\ldots} \tag{2.21}$$

In this equation t are the cluster amplitudes and $\hat{\tau}$ are the excitation operators. In a CC calculation, the cluster amplitudes have to be determined.

The coupled cluster methods form a hierarchy, whose members are denoted by the n-particle excitation operators used in the calculation. Including only single and double excitations leads to CCSD. The Taylor-series expansion of the cluster operator for CCSD becomes:

$$\begin{aligned} e^{\hat{T}_1+\hat{T}_2} = 1 \quad &+ \quad \hat{T}_1 && (2.22)\\ &+ \quad \frac{1}{2!}\hat{T}_1^2 + \hat{T}_2 && (2.23)\\ &+ \quad \frac{1}{3!}\hat{T}_1^3 + \hat{T}_1\hat{T}_2 && (2.24)\\ &+ \quad \cdots && (2.25) \end{aligned}$$

The cluster operator contains single and double excitations, as well as higher products of these. These higher products are also known as connected clusters. In principle CCSD includes all excitations as connected clusters. The amplitudes for higher excitations (from connected clusters) are not optimised, therefore CCSD is not exact.

Coupled cluster calculations are size extensive but normally not variational. They can in principle be made variational, but the results do not justify the enormous effort.[23] The CC series converges rather fast. The expressions for CC gradients and response functions are somewhat involved. CC calculations are also expensive. One way to improve the results is to include higher excitations as a perturbation leading e.g. to the CCSD(T) method, where the unconnected triple excitations are

calculated as a perturbation. CCSD(T) with a triple-zeta basis set often gives excellent results, close to chemical accuracy (a few kJ/mol). However, the method still builds on a single reference (one Slater determinant) and can therefore not be used to describe bond breaking. Kowalski and co-workers proposed a renormalised CC method which should be able to describe also bond-breaking.[24] In recent years a lot of effort has been put into the development of a multi-reference CC theory.[25] Such a formalism would circumvent the problems inherent to single-reference approaches.

To lower the computational effort of coupled cluster calculations, approximative cluster equations can be used. A hierarchy of coupled-cluster methods developed to facilitate the calculation of molecular properties uses such approximative cluster equations. These are referred to as CC2, CC3 ... CCn methods.[26]

Both MP2 and CCSD/CC2 often give rather good results. One reason for that is, that double excitations account for 90% of the correlation contribution. Single excitations as included in CCSD/CC2 account for orbital relaxation. The orbitals used in CCSD/CC2 calculations are the optimised Hartree-Fock orbitals and not correlated orbitals, therefore the orbitals have to be relaxed to describe the correlated system.

There are several definitions of norms in CC theory that help to establish whether a system is treated sufficiently well with a single determinant. This is done by calculating the maximum contribution of single excitations. If they are high, then multi-reference methods should be used (see below). One of these diagnostics which is often used is the T_1 diagnostic of Taylor and coworkers.[27]

A completely different approach to treat electron correlation was proposed by Schirmer et al. in 1983.[28] Their method, the algebraic diagrammatic construction (ADC) uses a diagrammatic perturbation expansion of Green's function. It was recently shown, that the formulas derived by that approach are very similar to the formulas from the CC method.

2.2.4 Configuration Interaction

The MPn and CC methods described above have one feature in common. They add excitations to the ground state wavefunction to account for electron correlation. The simplest way to do that, would be to add weighted Slater determinants of excited states to the ground state:

$$\Psi_{CI} = a_0\Phi_{SCF} + \sum_S a_S\Phi_S + \sum_D a_D\Phi_D + \sum_T a_T\Phi_T + \dots \tag{2.26}$$

where S,D and T stands for singlet, doublet and triplet excitations respectively. The added excited states are, in fact, often linear combinations of Slater determinants. This can be necessary to make them proper spin eigenfunctions. Such a linear combination is called a configuration state function (CSF).

An advantage of this treatment is, that the resulting method is variational. As stated earlier, double excitations account already for most of the correlation energy, therefore CISD was a widely used method. The method has the problem of not being size consistent. Size consistency means, that the energy of non interacting systems at a large distance should be the sum of the energy of the seperate systems. This is an important feature e.g. when calculating dissociation energies.

Full CI calculations include all possible excitations for a given molecule in a given basis. These calculations are extremely expensive and can be done only for the smallest molecules. Even for small molecules, such as N_2, billions of CSF's are needed.[29] FCI calculations are still important as benchmarks. The full CI wavefunction can be used to get CC and MPn results to arbitrary order. The FCI method is also size consistent.

It was shown, that CISDTQ recovers almost all of the correlation energy and minimises the size consistency error dramatically.[30] Such calculations are already rather expensive, so Davidson devised a method to estimate the contributions of quadruple excitations[31] in order to reduce the size consistency error of CISD calculations. This Davidson correction is often used when CISD calculations are performed.

$$\Delta E_Q \approx (1 - a_0^2)(E_{CISD} - E_{SCF}) \tag{2.27}$$

A CI method that is exactly size-consistent is the quadratic CISD (QCISD).[32] It can be viewed as an extension of CI or a simplification of CCSD retaining size consistency. Helgaker et al. found, that CISD gives rather poor results compared to other correlated methods.[33] Because of this and because of often appearing convergence problems, CI calculations have almost lost their importance, except for benchmarking calculations.

2.2.5 Multi-Reference Methods

When one wishes to calculate parts of the potential hypersurface away from a minimum accurately, single-reference methods will often fail, as occupancy of the orbitals might change significantly. Neither will single-reference methods work for systems with very low-lying excited states. In such cases multi-reference methods have to be used. The most straightforward way to do so is a multi-configuration self-consistent field (MCSCF) calculation. In an MCSCF calculation not only the weight factors of Equation (2.26) are optimised but also the expansion coefficients of the molecular orbitals, that make up the CSF's, are optimised. The resulting procedure is similar to an HF-SCF procedure.

A special type of MCSCF calculations is the CASSCF (complete active space SCF) method of Roos and coworkers.[34] Here one defines an active space containing occupied and unoccupied orbitals. In this active space all configuration state functions are constructed and then an MCSCF calculation with these CSF's is performed. The computational effort for CASSCF calculations increases dramatically with the number of orbitals in the active space. 15 electrons in 15 orbitals is about the limit at the moment. The results of CASSCF calculations can still be improved, by adding dynamical correlation to the CASSCF wavefunction. If in the method of Roos et al. MP perturbation theory is used on the CASSCF wavefunction, the resulting method is coined CASPTn.[35] Mostly corrections to second order are included (CASPT2). This method gives highly accurate results even for complicated systems as U_2.[36]

2.2.6 Density Functional Theory

In 1964 Hohenberg and Kohn proved a theorem whose application led to one of the most widely used computational methods. They showed, that the ground state energy and all ground-state properties are uniquely determined by the ground state electron density.[37,38] As the electron density is a function of three spatial coordinates, the energy is a functional of the density E[ρ]. This is quite an intriguing statement. The wave function for an n-electron system depends on 3n spatial coordinates, while according to Hohenberg and Kohn 3 spatial coordinates are enough.

To make this into a useful computational theory, we need the second Hohenberg and Kohn theorem, the variational theorem. It states, that the true ground state electron density minimises the energy functional (similar to the variational method in wave function theory, which states, that the true wavefunction minimises the energy). Originally these two theorems were only proven for non-degenerate ground states, but Levy extended them to degenerate ground states.[39]

Nice as these theorems are, they do not tell us how to get the electron density of a system without first calculating the wave function. Neither do they describe how to get the energy from the density. The energy functional can be split up in the following way:

$$E_0 = E_v[\rho_0] = \overline{T}[\rho_0] + \overline{V}_{Ne}[\rho_0] + \overline{V}_{ee}[\rho_0] \tag{2.28}$$

The nucleus-electron interaction functional,

$$\overline{V}_{Ne} = \int \rho_0(\mathbf{r}) v(\mathbf{r}) d\mathbf{r} \tag{2.29}$$

is known, but the other two are not. They have to be approximated. While DFT in principle is an exact method, it delivers only approximative results, because the kinetic-energy functional and the electron-interaction functional are not exactly known.

Kohn and Sham developed DFT further to facilitate the approximation of the elusive functionals.[40] They considered a system of non-interacting particles in an external potential $v_s(\mathbf{r}_i)$ (where the subscript s denotes the non-interacting system). This potential is chosen so, that the ground-state density

of this system equals the density of the real interacting system. As the electrons do not interact the Hamiltonian can be written as:

$$\hat{H}_s = \sum_{i=1}^{n}[-\frac{1}{2}\nabla_i^2 + v_s(\mathbf{r}_i)] \equiv \sum_{i=1}^{n}\hat{h}_i^{KS} \tag{2.30}$$

With this equation we can construct one particle Kohn-Sham orbitals.

$$\hat{h}_i^{KS}\theta_i^{KS} = \epsilon_i^{KS}\theta_i^{KS} \tag{2.31}$$

Kohn and Sham then went on to rewrite the energy equation as follows. For the kinetic energy functional one gets:

$$\Delta\overline{T}[\rho] \equiv \overline{T}[\rho] - \overline{T}_s[\rho] \tag{2.32}$$

and for the electron interaction:

$$\Delta\overline{V}_{ee}[\rho] \equiv \overline{V}_{ee}[\rho] - \frac{1}{2}\int\int\frac{\rho(\mathbf{r}_1)\rho(\mathbf{r}_2)}{r_{12}}d\mathbf{r}_1 d\mathbf{r}_2 \tag{2.33}$$

With these definitions the energy functional becomes

$$E_v[\rho] = \int\rho_0(\mathbf{r})v(\mathbf{r})d\mathbf{r} + \overline{T}_s[\rho] + \frac{1}{2}\int\int\frac{\rho(\mathbf{r}_1)\rho(\mathbf{r}_2)}{r_{12}}d\mathbf{r}_1 d\mathbf{r}_2 + \Delta\overline{T}[\rho] + \Delta\overline{V}_{ee}[\rho] \tag{2.34}$$

The two last terms in this equation are unknown and are combined to form the exchange-correlation energy functional:

$$E_{xc} \equiv \Delta\overline{T}[\rho] + \Delta\overline{V}_{ee}[\rho] \tag{2.35}$$

With the help of Kohn-Sham orbitals we can evaluate the energy functional expression above if the exchange-correlation energy functional is known. A lot of effort has been put into finding good approximations for E_{xc}. An early example is the local density approximation of Hohenberg and Kohn which holds when the density varies slowly over space.

$$E_{xc}^{LDA}[\rho] = \int\rho(\mathbf{r})\varepsilon_{xc}(\rho)d\mathbf{r} \tag{2.36}$$

Here $\varepsilon_{xc}(\rho)$ is the exchange-correlation energy of an electron in a uniform electron gas of density ρ. This model is also known as 'jellium'. LDA works quite well in solid state calculations. Even for molecules, where ρ varies rapidly over space, LDA gives surprisingly good results for molecular geometries and vibrational frequencies. LDA gives very poor results for properties like atomization energies. Improvements on LDA are therefore necessary. Spin can be included in LDA, the resulting method is known as LSDA (a popular LSDA functional is SVWN[41]).

One way to improve on LSDA is the inclusion of the gradient of the density to allow for fast-varying electron densities. This is known as the generalised gradient approximation (GGA).[42] Splitting the exchange-correlation energy functional in an exchange and a correlation part, exchange and correlation functionals have been developed. Hartree-Fock exchange can be added (also known as exact exchange) this leads to the so called hybrid functionals like the immensely popular B3LYP.[43]

The number of functionals available is staggering. Some of them are fitted to experimental parameters (like B3LYP) and could therefore be called semi-empirical. For a given system the functionals sometimes perform somewhat randomly. This has led to certain conflicts between groups preferring certain functionals. Such quarrels have slightly tainted the lustre of DFT.

Present day functionals have certain problems that shall be mentioned briefly. The double integral in Equation (2.34) contains a self interaction which would be exactly cancelled by the correct E_{XC}. Currently available functionals have problems with that. The SIC (self interaction corrected) functionals have other problems making their usage difficult. Dispersion-type interactions are difficult to describe

with the available functionals. Charge-transfer excitations are sometimes a problem for DFT. Finally, it is somewhat difficult to build up a hierarchy like in CC or MP calculations to systematically improve the results of DFT calculations.

A very interesting proposal by Perdew is the so called Jacob's ladder approach by which one can systematically improve on functionals, by adding 'new physics' step by step.[44] The lowest rung on this ladder is using the local density (LDA). The next rung adds the gradient of the density (GGA). The third rung includes the kinetic energy density (meta-GGA). The next step would be to design functionals which are defined in terms of the occupied KS orbitals (nonlocal functionals).

Despite the practical problems of DFT, the method has developed into the most widely used technique in computational chemistry.

2.2.7 Scaling

To conclude the exploration of the x-axis in Figure 2.1, we shall look at the scaling of the methods presented above and briefly mention ways to reduce the scaling. Table 2.1 shows the scaling of some methods.

Method	Scaling
non-hybrid DFT	N^3
Hartree-Fock	N^4
MP2	N^5
CCSD	N^6
MP4,CCSD(T)	N^7
...	
FCI	N!

Table 2.1: Scaling of some computational methods with basis set size N

Non-hybrid DFT actually scales better than Hartree-Fock, although the DFT method contains electron correlation. This is of course one of the reasons, why DFT is so immensely popular. Recent years have seen a lot of development to reduce scaling. The ultimate goal would be to achieve linear scaling with system size. A widely employed method to reduce the scaling is the use of density fitting. In this method the electron density is expanded in a set of auxiliary basis-functions. The density is then used to compute the Coulomb part of non-hybrid functionals. With this method, also known as RIDFT (RI=resolution of the identity) the computational time can be reduced by an order of magnitude. RI techniques can be used for correlated methods as well (RIMP2, RICC2).

2.3 The Hamiltonian

In this section we shall look at how the choice of Hamiltonian changes the accuracy of a calculation. Special emphasis shall be put on the inclusion of relativistic effects. One fact should be noted in the beginning. The choice of Hamiltonian does not change the scaling of the method. It appears as a factor in front of the scaling. Admittedly, this factor can become rather large.

2.3.1 Relativistic Mechanics

The theory of special relativity was developed by Einstein in the beginning of the last century.[45] It usually adds a small correction to classical physics and becomes important when particles move at velocities close to the speed of light (relativistic velocities). This is in fact the case for electrons in the vicinity of heavy nuclei, e.g. the 1s electrons of heavy elements. The average speed of an 1s electron in the non-relativistic limit is Z in atomic units. The v/c ratio for the gold 1s electrons thus becomes $79/137 = 0.577$. This means that this electron moves with 58 % of the speed of light. A relativistic treatment is therefore necessary in this case.

Equations in classical mechanics have to be covariant under the Galilei transformation. In relativistic mechanics, they have to be covariant under a Lorentz transformation. The Lorentz transformations treat time and space on equal footing, in fact they can be seen as a rotation in four-dimensional space time. This means, that a relativistic wave equation has to treat space and time on equal footing as well. The time-dependent Schrödinger equation does not fulfil this requirement and is clearly not Lorentz covariant.

2.3.2 Relativistic Wave Equations

To derive a relativistic wave equation we can use the relativistic energy expression

$$\begin{aligned} E^2 - p^2c^2 &= \frac{(m_0c^2)^2}{1-\frac{v^2}{c^2}} - c^2\frac{m_0^2v^2}{1-\frac{v^2}{c^2}} \\ &= (m_0c^2)^2 \end{aligned} \tag{2.37}$$

Replacing classical mechanical quantities by quantum mechanical operators yields

$$-\hbar^2\frac{\partial^2\Psi(x,t)}{\partial t^2} = \left[-\hbar^2c^2\nabla^2 + m_0^2c^4\right]\Psi(x,t) \tag{2.38}$$

This is the well known Klein-Gordon equation for a free particle in the absence of external fields.[46,47] It treats time and space on equal footing and it can be shown to be Lorentz covariant. The Klein-Gordon equation is second order in both time and space. This can lead to negative charge densities at some points in space, a feature that is not very desirable. One would therefore like to find a wave equation that is linear in time and space.

2.3.3 The Dirac Equation

Dirac derived his wave equation by requiring that it should be linear in space and time and that the solution for the free particle should equal the solutions of the Klein-Gordon equation.[48] It became apparent that the requirements would lead to an equation with more than one component. Starting from a linear equation of the form:

$$\left(-\frac{1}{c}\frac{\hbar}{i}\frac{\partial}{\partial t} - \boldsymbol{\alpha}\hat{\mathbf{p}} - \beta m_0c\right)\Psi = 0 \tag{2.39}$$

and multiplying this equation with its complex conjugate, one can see that the resulting equation is equal to the Klein-Gordon equation if the following permutation relations are fulfilled

$$[\alpha_i, \alpha_j]_+ = \alpha_i\alpha_j + \alpha_j\alpha_i = \delta_{ij} \tag{2.40}$$

with i and j going from zero to three and $\alpha_0 = \beta$. Evaluating these relations, one can show that the smallest possible number of components is four. The well known Pauli spin matrices :

$$\sigma_1 = \begin{pmatrix} 0 & 1 \\ 1 & 0 \end{pmatrix} \qquad \sigma_2 = \begin{pmatrix} 0 & -i \\ i & 0 \end{pmatrix} \qquad \sigma_3 = \begin{pmatrix} 1 & 0 \\ 0 & -1 \end{pmatrix} \tag{2.41}$$

can be used to construct α and β. This leads to:

$$\beta = \alpha_0 = \begin{pmatrix} I_{2\times2} & 0 \\ 0 & -I_{2\times2} \end{pmatrix} \tag{2.42}$$

$$\alpha_i = \begin{pmatrix} 0 & \sigma_i \\ \sigma_i & 0 \end{pmatrix} \qquad (i = 1-3) \tag{2.43}$$

Here $I_{2\times2}$ is the two by two unity matrix.

The Dirac equation is a set of coupled differential equations which can be written in the free particle case as

$$\begin{pmatrix} (\hat{p_0} - m_0c) & 0 & -\hat{p_z} & -(\hat{p_x} - i\hat{p_y}) \\ 0 & (\hat{p_0} - m_0c) & -(\hat{p_x} + i\hat{p_y}) & \hat{p_z} \\ -\hat{p_z} & -(\hat{p_x} - i\hat{p_y}) & (\hat{p_0} + m_0c) & 0 \\ -(\hat{p_x} + i\hat{p_y}) & \hat{p_z} & 0 & (\hat{p_0} + m_0c) \end{pmatrix} \begin{pmatrix} \psi_1 \\ \psi_2 \\ \psi_3 \\ \psi_4 \end{pmatrix} = 0 \tag{2.44}$$

with $\hat{p_0}$ beeing:

$$\hat{p_0} = -\frac{1}{c}\frac{\hbar}{i}\frac{\partial}{\partial t} \tag{2.45}$$

For nontrivial solutions, the determinant of the matrix in Equation(2.44) has to become zero. This leads to the following solutions for the energy:

$$E_{\pm} = \pm c\sqrt{\hat{p_x^2} + \hat{p_y^2} + \hat{p_z^2} + (mc)^2} \tag{2.46}$$

The negative energy solution was somewhat surprising until the discovery of the positron. According to Dirac's explanation, the electronic states with negative energy are completely filled (Dirac sea). It is possible to excite electrons from these negative-energy states, thus creating a hole in the Dirac sea. This hole can be seen as a particle with positive charge, the positron. The described process is known as pair creation. This success of his equation lead Dirac to his famous statement: "This equation is clearly more intelligent than I am." By a simple transformation, the energy scale can be aligned to the nonrelativistic case

$$\beta' = \begin{pmatrix} 0 & 0 \\ 0 & -2I_{2\times 2} \end{pmatrix} \tag{2.47}$$

An interesting property of the Dirac Hamiltonian is, that $\hat{l}$ and $\hat{s}$ no longer commute with the Hamiltonian. They are not good quantum numbers any more. Instead, a new quantum number $j = l + s$, which commutes with the Dirac Hamiltonian, is introduced.

The four-component wave function can be split into two two-component wave-functions:

$$\Psi = \begin{pmatrix} \phi \\ \chi \end{pmatrix} \tag{2.48}$$

where ϕ is called the large component and χ the small component. With these two components, the Dirac equation can be written as:

$$V\phi + c\boldsymbol{\sigma} \cdot \hat{\mathbf{p}}\chi = E\phi \tag{2.49}$$

$$c\boldsymbol{\sigma} \cdot \hat{\mathbf{p}}\phi + (V - 2c^2)\chi = E\chi \tag{2.50}$$

2.3.4 The n-Electron Dirac Hamiltonian

So far everything is exact. We have a relativistic wave equation in which we can, by the use of the gauge invariance, introduce external potentials. But the equation is a one-electron equation. For chemical systems this is not sufficient. The easiest way to construct an n-electron Hamiltonian would be to add a Coulomb repulsion term for the electron repulsion. The Coulomb term is unfortunately not Lorentz covariant. It treats the electron interaction as instantaneous, which is obviously incorrect in a relativistic picture. To treat the electron interaction correctly, one has to include QED effects. The resulting equation is called the Bethe-Salpeter equation.[49] It is an integralo-differential equation

which is very hard to solve. It has only been used for small atomic systems. An approximation exists in the Breit term[50]

$$V_{ee}^{\text{Coulomb-Breit}}(r_{12}) = \frac{1}{r_{12}} - \frac{1}{2r_{12}}\left[\boldsymbol{\alpha}_1 \cdot \boldsymbol{\alpha}_2 + \frac{(\boldsymbol{\alpha}_1 \cdot \mathbf{r}_{12})(\boldsymbol{\alpha}_2 \cdot \mathbf{r}_{12})}{r_{12}^2}\right] \tag{2.51}$$

It consists of the Coulomb-, Gaunt- and retardation term. The Gaunt and retardation terms cancel each other partly. It is therefore not advisable to include only the Gaunt term (although this is much easier computationally). It has turned out, that the error one makes in using only the Coulomb term is not so big. Therefore nowadays the Dirac-Coulomb Hamiltonian is mostly used in four-component calculations.

2.3.5 The Small Component

The computational effort of four-component calculations is quite high. One reason for this is that the basis set for the small component should be constructed from the basis set for the large component by kinetic balance, which is:

$$\chi = \frac{1}{2c^2 + E - V} c\boldsymbol{\sigma} \cdot \hat{\mathbf{p}}\phi \tag{2.52}$$

The momentum operator $\hat{\mathbf{p}}$ creates from an l-function in the basis set for the large component an l+1 and an l-1 function in the small-component basis set. The basis set for the small component is therefore much bigger than the basis set for the large component. This is especially unfortunate, because the small component is an extremely local property as can be seen in Figure 2.2

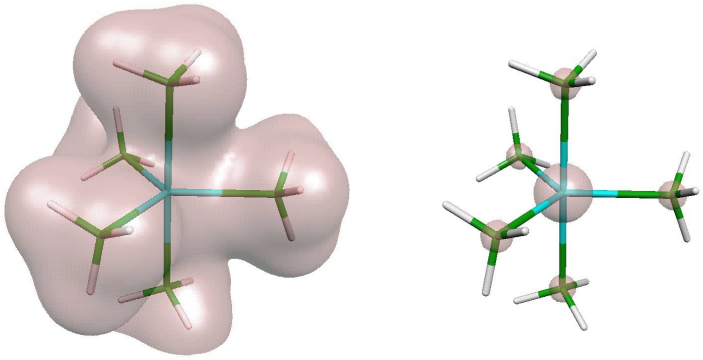

Figure 2.2: On the left, the large-component density of $Bi(CH_3)_5$. On the right, the small-component density 100 times magnified. Result of an all electron Dirac-Coulomb Hartree-Fock calculation, done by the author.

Clearly we would like to use some approximations to reduce the computational effort. The small component will be involved in LS and SS type integrals. A simple approximation that works quite well for energy differences and geometries is to leave out the SS integrals. A more correct approach is the one-centre approximation of Visscher[51] or the slightly different approach by Pedersen.[52] In these approaches the LS and SS integrals are replaced by an effective charge of the atom. A new method that seems to work very well is the use of density fitting in four-component calculations. This has recently been implemented in the BERTHA code.[53]

2.3.6 The Spin-free Dirac Hamiltonian

An interesting simplification of the Dirac equation is the elimination of the spin from it. This may sound strange, but it is an interesting tool to test if scalar relativistic effects or spin-orbit effects are predominant in a certain system.

Multiplying the Dirac equations with

$$2mc\chi = (\boldsymbol{\sigma}\cdot\hat{\mathbf{p}})\phi \tag{2.53}$$

gives the following set of equations:

$$(V-E)\chi + T\phi = 0 \tag{2.54}$$

$$T\chi + \left[\frac{1}{4m^2c^2}(\boldsymbol{\sigma}\cdot\hat{\mathbf{p}})(V-E)(\boldsymbol{\sigma}\cdot\hat{\mathbf{p}}) - T\right]\phi = 0 \tag{2.55}$$

Using the well known Dirac relation $((\boldsymbol{\sigma}\cdot\hat{\mathbf{u}})(\boldsymbol{\sigma}\cdot\hat{\mathbf{v}}) = \hat{\mathbf{u}}\cdot\hat{\mathbf{v}} + i(\boldsymbol{\sigma}\cdot\hat{\mathbf{u}}\times\hat{\mathbf{v}}))$ on this set of equations leads to

$$\tilde{h}_D = \begin{pmatrix} V & T \\ T & \frac{1}{4m^2c^2}(\hat{\mathbf{p}}\cdot V\hat{\mathbf{p}}) - T \end{pmatrix} + \begin{pmatrix} 0 & 0 \\ 0 & \frac{1}{4m^2c^2}i(\boldsymbol{\sigma}\cdot(\hat{\mathbf{p}}V)\times\hat{\mathbf{p}}) \end{pmatrix} \tag{2.56}$$

The first term in this equation is the spin-free Hamiltonian.[54] Note that this transformation also leads to a change in the metric. The spin-free Hamiltonian can be used self consistently and is implemented in the programme package DIRAC.[55] As the DIRAC code uses time-reversal symmetry (Kramers-restricted calculations) this Hamiltonian cannot be used with time-antisymmetric (magnetic) operators.

2.3.7 Pauli and Breit-Pauli Hamiltonian

The relation between the small and the large component can be used to eliminate the small component from the wave equation. The resulting ESC (elimination of the small component) equation is no longer a proper eigenvalue equation since the eigenvalue (the energy) is included in the operator

$$\chi = \frac{1}{2c^2 + E - V}c\boldsymbol{\sigma}\cdot\hat{\mathbf{p}}\phi \tag{2.57}$$

It is nevertheless useful for perturbative treatment. If the prefactor of the equation above is slightly rewritten:

$$\frac{1}{2c^2+E-V} = (2c^2)^{-1}\left(1 + \frac{E-V}{2c^2}\right)^{-1} = (2c^2)^{-1}K \tag{2.58}$$

and the result inserted into the ESC equation, one gets

$$\hat{H}_D^{esc} = V + \frac{1}{2m}\boldsymbol{\sigma}\hat{\mathbf{p}}K\boldsymbol{\sigma}\hat{\mathbf{p}} \tag{2.59}$$

Expansion of K (normal expansion) leads to the Pauli equation

$$K = \left(1 + \frac{E-V}{2c^2}\right)^{-1} \approx 1 - \frac{E-V}{2c^2} + \cdots \tag{2.60}$$

In zeroth order this equation gives the nonrelativistic limit. Going to first order leads to the Pauli Hamiltonian. This is a computationally easy way to treat relativistic effects. The biggest problem with this approach is, that the assumption made in rewriting K (namely that $E-V$ is small compared to $2c^2$) does not hold everywhere in a central potential. Furthermore it is singular at the nucleus and only usable as a perturbation.

If electron interactions are treated with the Breit equation, one can transform the resulting Dirac equation by a Foldy-Wouthuysen transformation to get the Breit-Pauli Hamiltonian. This Hamiltonian is in principle plagued by the same problems as the Pauli Hamiltonian. It contains a number of terms which can be attributed to different relativistic effects. The Breit-Pauli Hamiltonian can be written as

$$H_{BP} = H_1 + H_2 + H_3 + H_4 + H_5 + H_6 + H_7 \tag{2.61}$$

where the different terms for a many-electron atom are given by:

$$H_1 = \sum_i \left(\frac{1}{2m_0} p_i^2 - \frac{Ze^2}{r_i} \right) + \sum_j \sum_{i>j} \frac{e^2}{r_{ij}} \tag{2.62}$$

$$H_2 = -\frac{1}{8m_0^3 c^2} \sum_i p_i^4 \tag{2.63}$$

$$H_3 = -\frac{e^2}{2m_0^2 c^2} \sum_j \sum_{i>j} \left[\frac{\mathbf{p}_i \cdot \mathbf{p}_j}{r_{ij}} + \frac{(\mathbf{r}_{ij} \cdot \mathbf{p}_i)(\mathbf{r}_{ij} \cdot \mathbf{p}_j)}{r_{ij}^3} \right] \tag{2.64}$$

$$H_4 = \frac{\mu}{m_0 c} \sum_i \mathbf{s}_i \cdot \left\{ \mathbf{E}_i \times \mathbf{p}_i + \sum_j \sum_{i>j} \frac{2e}{r_{ij}^3} [\mathbf{r}_{ij} \times \mathbf{p}_j] \right\} \tag{2.65}$$

$$H_5 = \frac{ie\hbar}{4m_0^2 c^2} \sum_i (\mathbf{p}_i \cdot \mathbf{E}_i) \tag{2.66}$$

$$H_6 = 4\mu^2 \left\{ \sum_j \sum_{i>j} \left[\frac{\mathbf{s}_i \cdot \mathbf{s}_j}{r_{ij}^3} - 3\frac{(\mathbf{s}_i \cdot \mathbf{r}_{ij})(\mathbf{s}_j \cdot \mathbf{r}_{ij})}{r_{ij}^5} - \frac{8\pi}{3} (\mathbf{s}_i \cdot \mathbf{s}_j) \delta^3(r_{ij}) \right] \right\} \tag{2.67}$$

$$H_7 = 2\mu \sum_i (\mathbf{H}_i \cdot \mathbf{s}_i) + \frac{e}{m_0 c} \sum_i (\mathbf{A}_i \cdot \mathbf{p}_i) \tag{2.68}$$

The following abbreviations have been used:

$$\begin{aligned} E_i &= -\nabla_i V \\ V &= -\sum_i \frac{Ze^2}{r_i} + \sum_j \sum_{i>j} \frac{e^2}{r_{ij}} \\ \mu &= \frac{e\hbar}{2m_0 c} \\ \mathbf{p}_i &= -i\nabla_i \end{aligned}$$

For transperency, the equations above are given in Gauss-cgs units. The following interactions can be discerned in the Breit-Pauli Hamiltonian. Equation (2.62) is the nonrelativistic Schrödinger Hamiltonian for a many-electron system. Equation (2.63) is the so called mass-velocity term. It is caused by the relativistic mass increase of the electrons. Equation (2.64) describes the retarded interaction of the different electron-orbits (orbit-orbit coupling). Equation (2.65) is the spin-orbit coupling term. It contains spin-orbit and spin-other orbit contributions. Equation (2.66) is called the Darwin term. It accounts for the fact, that the electrons are slightly vibrating around their path (Zitterbewegung). The penultimate term (2.67) describes the spin-spin coupling of the electrons. Finally Equation (2.68) accounts for the interaction of the electrons with external electromagnetic fields. In this form the Hamiltonian is only valid for many-electron atoms. In order to generalise it to many-electron molecules, electron-nucleus and nucleus-nucleus interaction have to be added.

The terms present in the Breit-Pauli Hamiltonian can be used in a perturbation treatment to estimate the size of different relativistic contributions.

2.3.8 Regular expansions

The ESC equation above can be rewritten to

$$\hat{H}_D^{esc} = V + \frac{c^2}{2mc^2 - V} \boldsymbol{\sigma}\hat{\mathbf{p}} \left(1 + \frac{E}{2mc^2 - V} \right)^{-1} \boldsymbol{\sigma}\hat{\mathbf{p}} \tag{2.69}$$

When we now expand in powers of K'

$$K' = \left(1 + \frac{E}{2mc^2 - V}\right)^{-1} \tag{2.70}$$

we obtain to the regular expansions. This methods yields relativistic corrections already in zeroth order (ZORA). ZORA can be used variationally, it is not singular at the nucleus and it is bounded from below up to $Z = 137$. Going to first order yields FORA (first order regular expansion) which cannot be used variationally. Other methods using the regular expansion have been developed. A good review was recently given by Sundholm.[56]

2.3.9 Foldy-Wouthuysen and Douglas-Kroll Transformation

There is a number of schemes to reduce the four-component Dirac equation to a two component equation. Two of those shall be described here very briefly, starting with the Foldy-Wouthuysen transformation.[57] The idea is to decouple the Dirac equation with a unitary transformation of the form

$$U = \begin{pmatrix} \frac{1}{\sqrt{1+X^\dagger X}} & \frac{1}{\sqrt{1+X^\dagger X}} X^\dagger \\ -\frac{1}{\sqrt{1+XX^\dagger}} X & \frac{1}{\sqrt{1+XX^\dagger}} \end{pmatrix} \tag{2.71}$$

The U we are looking for should block diagonalise the Hamiltonian $\hat{H}_D$. The aim is to decouple ϕ and χ, i.e. to reduce the size of the off-diagonal elements in the Hamiltonian. $\hat{H}_D$ can be split up in odd and even parts. An exponential form of an operator is used as the transformation matrix

$$\hat{U} = e^{i\hat{S}} \qquad \hat{S} = -i\beta\frac{\alpha\hat{p}}{2c} \tag{2.72}$$

The Baker-Campbell-Hausdorff formula can be used to express the exponential. The terms of similar powers are collected as nested commutators. They are then split into odd and even terms. The largest odd term can then be removed. The resulting formulas are quite difficult. The Hamiltonian derived with this procedure has some peculiar properties, therefore the Foldy-Wouthuysen transformation is not used as such.

A similar, but more useful procedure is the Douglas-Kroll transformation.[58,59,60] As a start, a first order Foldy-Wouthuysen transformation in momentum space is done. The resulting Hamiltonian is split again in odd and even terms. Now a different transformation including anti-hermitian operators $\hat{W}$ is done

$$\hat{U}' = \sqrt{(1 + \hat{W}_1^2)} + W_1 \tag{2.73}$$

The operator can be chosen so that certain terms cancel. The resulting Hamiltonian is decoupled to the next order. This procedure can be continued to higher order. The resulting equations are again not trivial. It was recently shown, that the Douglas-Kroll Hamiltonian is well behaved and bounded from below.[61] It is normally only used as a correction to the one-electron integrals.

2.3.10 Valence-Electron Methods

Although scalar relativistic effects are most important for core electrons in absolute terms, chemists are more interested in the valence electrons. The energy of core orbitals is almost unchanged in a chemical reaction. For energy differences these are therefore not very important. This has led to the development of methods that deal with valence electrons only.

It turns out, that valence electron methods represent a very efficient way to introduce scalar relativistic effects. In these methods, the core electrons are either frozen or treated only as a potential. Figure 2.3 gives an overview of the available methods. In frozen-core calculations, all electron calculations on the atoms of the molecule are performed. From those atomic fragments, the molecule is built and in the molecular calculation, the core electrons are frozen. This procedure is used e.g. by the programme-package ADF.[62]

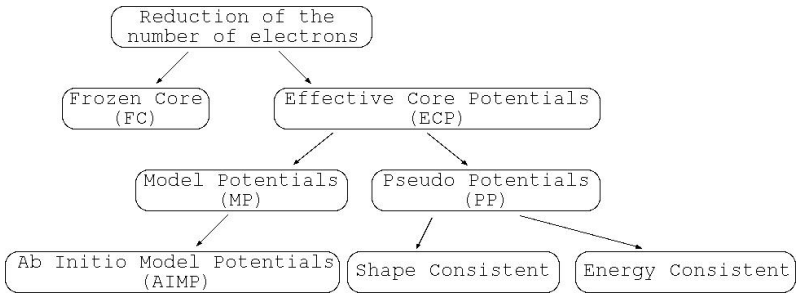

Figure 2.3: An overview of the available valence electron methods.

A different approach was already suggested in the late 1930s by the German quantum chemist Hellmann.[63] In this scheme, the inner electrons are replaced by an effective core potential (ECP).

As seen earlier, the Fock operator contains a sum over all electrons of differences of Coulomb and exchange integrals. This sum can be split up in a part for the valence electrons and a part for the core electrons. The inner electron interaction can be substituted by an effective potential. This gives an equation for the inner electron potentials

$$\hat{V}_l^{eff} = \epsilon_{eff} + \frac{Z_{eff}}{r} - \frac{l(l+1)}{2r^2} + \frac{\frac{1}{2}\nabla_r^2 - \hat{V}'_{val}\phi_i^l}{\phi_l^i} \tag{2.74}$$

In this equation ϕ_i may never be zero. Therefore the normal valence orbitals have to be replaced by node-free pseudo orbitals. These can be chosen to be shape consistent, that is they mimic the form of the real atomic orbitals. The inner part is described by a node free polynomial. The so constructed pseudo potentials are fitted to accurate atomic calculations using Hartree-Fock- or Dirac-Coulomb Hartree-Fock calculations.

It was earlier stated, that ECP's are only accurate if the core is small enough. Recent developments by Dolg et al. have led to large core ECP's for lanthanides[64] and actinides,[65] where the f-electrons are in the core. These potentials give rather accurate results while they reduce the computational demand substantially. Such ECP's have the advantage, that certain multireference problems like the Pu^{4+} ion can be treated with one component calculations, as the f electrons are in the core.

2.3.11 The Real Non-Relativistic Limit: The Lévy-Leblond Equation

As a last remark in this section the appearance of the electron spin shall be shortly discussed. The angular momentum is nonrelativistically given as

$$\mathbf{l} = \mathbf{r} \times \mathbf{p} \tag{2.75}$$

In a relativistic theory, 4-component space-time vectors have to be used. The resulting product tensor is of rank 4. This tensor contains the pure spatial components from nonrelativistic theory. There are also mixed spatial and temporal parts. An analysis of the space-time part of the angular momentum shows that it is actually independent of the centre of rotation, meaning that it represents an intrinsic property. This intrinsic property is the spin-angular momentum of the system.

The easiness with which the spin can be derived in a relativistic treatment has often led to the conclusion, that spin is a relativistic property. This is a statement that shall be discussed briefly now.

As mentioned earlier, the Schrödinger equation is Galilei covariant. As Dirac did for a relativistic wave equation, Lévy-Leblond linearised the Schrödinger equation.[66] The general ansatz used by him was

$$\theta = (AE + \mathbf{B} \cdot \hat{\mathbf{p}} + C) \tag{2.76}$$

The idea is then to find some θ' so that $\theta \cdot \theta'$ recovers the Schrödinger equation. The algebra needed is a bit more involved, but rewriting the equation above in 4-dimensional Clifford algebra leads to a 4-component equation containing Pauli matrices:

$$E\phi + (\boldsymbol{\sigma} \cdot \hat{\mathbf{p}})\chi = 0 \tag{2.77}$$
$$(\boldsymbol{\sigma} \cdot \hat{\mathbf{p}})\phi + 2m\chi = 0 \tag{2.78}$$

A detailed analysis shows, that wave equations for spin s particles must have at least $(2s{+}1)$ components. The equation above has two identical eigenvalues:

$$E = \frac{p^2}{2m} \tag{2.79}$$

In other words, the linearised equation above describes particles with spin 1/2. It can be shown, that it is Galilei covariant. When external fields are included, the Lévy-Leblond equation can be transformed into the Pauli equation. This completely non-relativistic theory predicts for spin 1/2 particles:

$$\mu = \frac{q}{2m}\sigma \qquad \rightarrow \qquad g_s = 2 \tag{2.80}$$

So the gyromagnetic ratio of the electron predicted by the non-relativistic Lévy-Leblond equation is the same as can be obtained from a relativistic treatment. The equation contains no spin-orbit or mass velocity terms, these are relativistic phenomena.

This result could also be interpreted as the fact that the Galilei group can accomodate spin. This means not necessarily, that spin is present in a non-relativistic treatment. It can be added afterwards. For an interesting discussion of this point see reference 67.

The Lévy-Leblond equation is valuable for comparison with relativistic results. It is implemented in the software package DIRAC.

2.4 The Basis Set

We shall now briefly discuss the third axis of the coordinate system in Figure 2.1, the basis set.

The need for basis sets arise, because we have to describe the molecular orbitals in the Fock equation. For very small, highly symmetric systems like atoms or diatomic molecules this description can be done by mapping the MO's numerically on a grid.[68,69] This sort of calculation is known as a numerical Hartree-Fock calculation. Efforts have been made to extend such methods to bigger systems, as e.g. in real-space DFT methods.[70]

For all other problems we need to express the unknown MO's in terms of known functions. The use of a linear combination of one-electron basis function to describe the molecular orbitals was first proposed by Roothaan.[71] With the use of the expansion

$$\Phi_i = \sum_{s=1}^{n} c_{si}\chi_s \tag{2.81}$$

the Hartree Fock equation becomes

$$\sum_s c_{si}\hat{F}\chi_s = \varepsilon_i \sum_s c_{si}\chi_s \tag{2.82}$$

Multiplication of this equation by χ_r^* and subsequent integration gives

$$\sum_{s=1}^{n} F_{rs}c_{si} = \sum_{s=1}^{n} S_{rs}c_{si}\varepsilon_i \tag{2.83}$$

With $F_{rs} = \langle\chi_r|\hat{F}|\chi_s\rangle$ and $S_{rs} = \langle\chi_r|\chi_s\rangle$. There are n such equations, with r running from 1 to n. F_{rs} and S_{rs} can be seen as elements of a matrix. Introducing a coefficient matrix with the elements c_{si} and a diagonal matrix ε with the orbital energies ε_i in the diagonal, this equation can be seen as a matrix equation

$$\mathbf{FC} = \mathbf{SC}\varepsilon \tag{2.84}$$

When the basis functions are orthogonalised, the overlap matrix $\mathbf{S}$ is transformed into a unit matrix. The use of matrix algebra simplifies the implementation of the Hartree-Fock procedure on a computer.

2.4.1 Types of Basis Functions

A logical choice for the basis functions is to use atomic orbitals. This is known as the LCAO-MO (linear combination of atomic orbitals to form molecular orbitals) method. One type of functions used are Slater-type orbitals (STO)

$$\chi_{\zeta,n,l,m}(r,\theta,\varphi) = NY_{l,m}(\theta,\varphi)r^{n-l}e^{-\zeta r} \tag{2.85}$$

STO's resemble the solution of the Schrödinger equation for hydrogen-like atoms. They have the right exponential behaviour, but they have no radial nodes. To describe atomic orbitals correctly, linear combinations of STO's have to be used. The number of STO's needed is rather small. The problem with STO's is, that the calculations of some molecular two-electron integrals cannot be performed analytically. There are programme packages like ADF that perform numerical integrations of STO's, but most other programmes use a different type of basis functions. These are known as Gaussian-type orbitals (GTO)

$$\chi_{\zeta,n,l,m}(r,\theta,\varphi) = NY_{l,m}(\theta,\varphi)r^{2n-2-l}e^{-\zeta r^2} \tag{2.86}$$

GTO's have no cusp at the nucleus and they fall off too fast. Therefore linear combinations of a lot more GTO's have to be used to describe the atomic orbitals correctly. The big advantage over STO's is, that analytical integrations of two electron integrals are easy. A product of gaussians is still a gaussian.

2.4.2 Classes of Basis Sets

As stated above, a number of STO's or GTO's is necessary to describe an atomic orbital correctly. Basis sets are classified according to their size. There are also certain hierarchies of basis sets developed by different groups of researchers.

The simplest form of basis sets employ one basis function per occupied orbital, These are known as minimal basis sets. They are far too small to deliver reliable results. An example of a minimal basis are the STO-nG basis sets of Pople and coworkers.[72] They use a number of gaussians fitted to one Slater-type function per occupied orbital. They are abbreviated as STO-nG, where n is the number of gaussians used to describe the Slater-type function.

To improve the quality, we can double the number of basis functions. The resulting basis sets are said to be of double-ζ quality (DZ). As chemists are mostly interested in valence properties, it can be economical to use more functions for the valence electrons than for the core electrons. The resulting sets are known as split-valence basis sets (SV). The basis-set size can be extended further to TZ, QZ, 5Z and so on. The use of more basis functions increases the flexibility of the basis set.

Another important aspect is the use of higher angular-momentum function in a basis set. This is important for two reasons. Firstly, these functions can be used as polarisation functions. Without polarisation functions a hydrogen atom would be described only by spherical s-functions. When the hydrogen atom is to form a bond in a molecule, the charge distribution will be no longer spherical, therefore higher angular-momentum functions are necessary to allow for polarisation of the hydrogen atom. Secondly, these higher angular momentum functions are necessary when electron-correlation methods are used. Electron correlation describes how electrons 'avoid' each other. They should be able to do so radially and angularly. For the radial part functions of the same angular momentum are sufficient, but for the angular part higher angular-momentum function have to be included.

For almost all purposes it is important to construct balanced basis sets. As described above, polarisation functions are important, but one should not include too many. If this is done, unphysical results

may be the consequence. A 5s4p3d2f1g can be said to be balanced, the higher angular momentum functions can sometimes be left out, although this should be tested from case to case.

One technique often used in constructing basis sets is contraction. A sum of primitive GTO's can be used to form a contracted GTO. Two different contraction schemes are used. In segmented contraction, the PGTO's are divided into segments and each segment is used to form a CGTO. This means each PGTO is used only once. In the other scheme, called general contraction, all PGTO's are used to form a CGTO, each CGTO is formed with a different set of contraction coefficients.

Examples of the latter type of contraction are the atomic natural orbital basis sets (ANO) of Almlöf and coworkers.[73] These have recently been integrated for all atoms in the MOLCAS code.[74,75] It might be considered a disadvantage of the PGTO's, that a rather large number of PGTO's is needed to reach basis-set convergence.

The Dunning type correlation consistent (cc) basis sets[76] are somewhat smaller than the ANO's. They are classified as aug-cc-pCVnZ. Here aug and the C are optional. Aug means that the basis set it augmented with diffuse functions, the p stands for the inclusion of polarisation functions. VnZ means valence n-ζ. Finally the C means that the basis set is augmented by steep functions. The resulting basis sets form a hierarchy, one can systematically improve the accuracy by using higher n. This feature can be used to extrapolate to the basis set limit, or at least to the next order n.

An effective class of basis sets that employs the segmented contraction scheme are the ones from the Ahlrichs group.[77] The generic name for these is nZVP. The n again means that the basis set is off n-ζ quality. There may be more than one letter P. Each P standing for one set of polarisation functions. These basis sets are implemented in TURBOMOLE[78] and as most other basis sets they are freely available on the net.[79]

What are the basis-set needs for different calculations? For DFT calculations the basis-set limit is reached rather fast. For ground state energies a triple-ζ basis set with polarisation functions is normally good enough. For correlated methods like MP2 or coupled cluster, the basis-set limit is reached much later, one has to go to basis sets of quadruple-ζ quality or higher.

For the calculation of certain properties, special basis-set requirements exist. For nuclear shieldings, electrons close to the nucleus are important, therefore the basis set must contain extra steep functions. The calculation should be repeated, possibly on a small test system, until basis-set convergence is reached. To calculate electronic excitations a good description of diffuse unoccupied orbitals (into which the excitation takes place) is needed. Therefore one should add diffuse functions to the basis set until the basis-set limit is reached. There exists a strategy to optimise the basis set especially in the region of interest for a certain property. There is even a computer programme available for this task.[80] This short discussion shows, that special care is needed when properties are to be calculated. Property calculations will be discussed in more detail in the next section.

2.5 Molecular Properties

Often one is not only interested in calculating the energy of a system, but in the calculation of molecular properties like geometries, vibrational frequencies, excitation energies or nuclear shielding parameters to name a few. The calculation of molecular properties requires special methods, a few shall be shortly discussed below.

2.5.1 Perturbative Treatment

Most molecular properties can in principle be seen as a perturbation of the energy. The energy of the system can be expanded in the perturbation strength λ

$$E(\lambda) = E(0) + \frac{\partial E}{\partial \lambda}\lambda + \frac{1}{2}\frac{\partial^2 E}{\partial \lambda^2}\lambda^2 + \frac{1}{6}\frac{\partial^3 E}{\partial \lambda^3}\lambda^3 + \cdots \tag{2.87}$$

When λ is e.g. the change of nuclear coordinates then the first derivative is the molecular gradient, the second derivative is the molecular Hessian matrix (the force constants) and the third derivative is the tensor containing the anharmonic corrections.

This treatment can be extended, to include different perturbations and then the expansion above contains mixed derivatives as well. If one is interested in the IR absorption intensities, then one would have to calculate the derivative with respect to the electric field and the nuclear positions. The Raman intensities involve the second derivative with respect to the electric field and the first derivative with respect to the nuclear positions.

There exist several methods to calculate the terms in the expansion series. One method is the use of perturbation theory. A perturbative treatment yields for first and second order properties C_1 and C_2

$$C_1 = \lambda\langle\Psi_0 \mid \mathbf{P_1} \mid \Psi_0\rangle \tag{2.88}$$

$$C_2 = \lambda^2\left[\langle\Psi_0 \mid \mathbf{P_2} \mid \Psi_0\rangle + \sum_{i\neq 0}\frac{\langle\Psi_0 \mid \mathbf{P_1} \mid \Psi_i\rangle\langle\Psi_i \mid \mathbf{P_1} \mid \Psi_0\rangle}{E_0 - E_i}\right] \tag{2.89}$$

where the perturbation is described by linear and quadratic operators $\mathbf{P_1}$ and $\mathbf{P_2}$ respectively. First-order properties are simply the expectation value of $\mathbf{P_1}$ of the unperturbed wavefunction. The second-order equation contains a sum over all excited states and is difficult to evaluate for *ab initio* wavefunctions.

An alternative approach is the use of the coupled perturbed Hartree-Fock (CPHF) method for obtaining the first-order orbital response. Writing the matrix form of the Hartree-Fock equations for the unperturbed system

$$\mathbf{F}^0\mathbf{C}^0 = \mathbf{S}^0\mathbf{C}^0\varepsilon^0 \tag{2.90}$$

We can then expand $\mathbf{F}$,$\mathbf{C}$,$\mathbf{S}$ and ε in terms of the perturbation and collect terms of expansion of the same power. This gives for first order perturbations

$$\mathbf{F}^1\mathbf{C}^0 + \mathbf{F}^0\mathbf{C}^1 = \mathbf{S}^1\mathbf{C}^0\varepsilon^0 + \mathbf{S}^0\mathbf{C}^1\varepsilon^0 + \mathbf{S}^0\mathbf{C}^0\varepsilon^1 \tag{2.91}$$

$$(\mathbf{F}^0 + \mathbf{S}^0\varepsilon^0)\mathbf{C}^1 = (\mathbf{F}^1 + \mathbf{S}^1\varepsilon^0 + \mathbf{S}^0\varepsilon^1)\mathbf{C}^0 \tag{2.92}$$

These equations are called the coupled perturbed Hartree-Fock equations. For each perturbation one CPHF equation has to be solved. This is often done simultaneously.

2.5.2 Propagator Methods

Green's functions can be used to express the time dependent evolution of a given property of a system. The resulting propagator for two time dependent operators $\hat{A}(t)$ and $\hat{V}(t)$ can be written as

$$\langle\langle\hat{A}(t);\hat{V}(t')\rangle\rangle = -i\theta(t-t')\langle\Psi_0|\hat{A}(t)\hat{V}(t')|\Psi_0\rangle \pm i\theta(t'-t)\langle\Psi_0|\hat{V}(t)\hat{A}(t')|\Psi_0\rangle \tag{2.93}$$

To get the frequency representation of this propagator, it has to be Fourier transformed.

$$\langle\langle\hat{A};\hat{V}^\omega\rangle\rangle_\omega = \sum_{n=0}\frac{\langle\Psi_0|\hat{A}|\Psi_n\rangle\langle\Psi_n|\hat{V}^\omega|\Psi_0\rangle}{\omega - (E_n - E_0)} - \sum_{n=0}\frac{\langle\Psi_0|\hat{V}^\omega|\Psi_n\rangle\langle\Psi_n|\hat{A}|\Psi_0\rangle}{\omega + (E_n - E_0)} \tag{2.94}$$

This is also known as a linear response function, in this case the polarisation propagator. It yields excitation energies, transition moments and static polarisabilities ($\omega \to 0$). Another interesting propagator is the electron propagator (addition or removal of an electron). It gives the electron affinity and the ionisation potential. Higher order properties can be obtained from higher order response functions.

With the use of commutators the linear response function can be rewritten as:

$$\langle\langle\hat{A}(t);\hat{V}(t')\rangle\rangle = -i\theta(t-t')\langle\Psi_0|[\hat{A}(t),\hat{V}(t')]|\Psi_0\rangle \tag{2.95}$$

Now we use the Heisenberg equation of motion on the propagator and return to the frequency representation. The propagator can then be written as a series of commutators:

$$\langle\langle \hat{A}; \hat{V} \rangle\rangle = \omega^{-1} \langle \Psi_0 | [\hat{A}, \hat{V}] | \Psi_0 \rangle + \omega^{-2} \langle \Psi_0 | [\hat{A}, [\hat{H}, \hat{V}]] | \Psi_0 \rangle + \cdots \tag{2.96}$$

This leads to the super-operator formulation and transforms the equation to

$$\langle\langle \hat{A}; \hat{V} \rangle\rangle = \langle \Psi_0 | [\hat{A}, (\omega \mathbf{I} - \mathbf{H})^{-1} \hat{V}] | \Psi_0 \rangle \tag{2.97}$$

An inner projection onto a complete set of excitation/deexcitation operators ($\hat{h}$) leads to

$$\langle\langle \hat{A}; \hat{V} \rangle\rangle = (\hat{A}|\hat{h})(\hat{h}|\omega \mathbf{I} - \mathbf{H}|\hat{h})^{-1}(\hat{h}|\hat{V}) \tag{2.98}$$

For the polarisation propagator $\hat{h}$ contains terms $\hat{h}_2$,$\hat{h}_4$ $\hat{h}_6$ and so on; $\hat{h}_2$ e.g. generates single excitations and deexcitations. Taking only $\hat{h}_2$ into account yields the so called random phase approximation (RPA) for the calculation of excitation energies.

The linear response equation in the random phase approximation takes the following form:

$$\langle\langle \hat{A}; \hat{V}^{\omega} \rangle\rangle_{\omega} = -\mathbf{E}_A^{[1]^{\dagger}} \left(\mathbf{E}^{[2]} - \omega \mathbf{S}^{[2]} \right)^{-1} \mathbf{E}_V^{[1]} \tag{2.99}$$

where $\mathbf{E}_A^{[1]^{\dagger}}$ and $\mathbf{E}_V^{[1]^{\dagger}}$ are the property gradients, $\mathbf{E}^{[2]}$ the second derivative matrix and $\mathbf{S}^{[2]}$ the metric. The resolvent in this equation is difficult to invert. An iterative approach is used instead.

$$\left(\mathbf{E}^{[2]} - \omega \mathbf{S}^{[2]} \right) \mathbf{X} = -\mathbf{E}_V^{[1]} \tag{2.100}$$

Using a set of trial vectors for $\mathbf{X}$

$$\mathbf{X} = \sum_{i=1} b_i a_i \tag{2.101}$$

We then have to solve the n-dimensional reduced equations iteratively.

$$\left(\tilde{\mathbf{E}}^{[2]} - \omega \tilde{\mathbf{S}}^{[2]} \right) \mathbf{X} = \tilde{\mathbf{E}}_V^{[1]} \tag{2.102}$$

In a relativistic four-component formulation, these equations are normally complex.[81] In static cases they are reduced to real equations, due to the hermiticity of the involved operators. Relativistic perturbations are of the following general form

$$\hat{V} = -e\phi I_4 + ec(\boldsymbol{\alpha} \cdot \mathbf{A}) \tag{2.103}$$

2.5.3 Charges and Bonding Analysis

Chemists are often interested in how parts of a molecule are charged. There is unfortunately no unique way to determine the distribution of the electrons in a molecule. Partial charges are not observable quantities. But there is a number of schemes for calculating atomic charges and for partitioning of the electrons.

Probably oldest and most criticised is the Mulliken population analysis. We can write the numbers of electrons as the trace of the product of the overlap matrix with the density matrix:

$$N = \mathrm{Tr}(\mathbf{DS}) \tag{2.104}$$

where the density matrix is obtained from the occupied molecular orbitals as:

$$D_{\alpha\beta} = \sum_i c_{\alpha i} c_{\beta i} \tag{2.105}$$

A diagonal element of the $\mathbf{DS}$ matrix can be interpreted as the number of electrons in a certain AO. An off-diagonal element can be seen as half the number of electrons shared between two AO's.

The electrons shared between two AO's are taken to be shared equally between them. With these definitions, the electron population of atom A can be defined as

$$\rho_a = \sum_{\alpha \epsilon A}^{AO} \sum_{\beta}^{AO} D_{\alpha\beta} S_{\alpha\beta} \tag{2.106}$$

The net charge is then the nuclear charge minus the electron population. Problems of the Mulliken population analysis include non conservation of molecular multipole moments and erratic results for basis sets with many diffuse functions. The number of elements in a certain AO might even be bigger than two and the off-diagonal elements can be negative. A slight improvement, especially for the last two problems is presented by the Löwdin population analysis. Instead of the $\mathbf{DS}$ matrix it uses the $\mathbf{S^{1/2}DS^{1/2}}$ matrix. This matrix is diagonal with only zeros or twos as diagonal elements (or ones in the case of open-shell systems).

A different approach to arrive at partial charges are the Hirshfeld charges.[82] They are defined as

$$q_i = Z_i - \int \frac{\rho_i^{at}(r)\rho^{mol}(r)}{\sum_i \rho_i^{at}(r)} dv \tag{2.107}$$

Here Z_i is the nuclear charge and $\rho_i^{at}(r)$ spherically averaged ground-state atomic density of atom i in the molecule and $\rho^{mol}(r)$ is the molecular electron density. This concept can be extended to fragments consisting of several atoms. It is quite useful for describing the shift in electron density upon the formation of the molecule.

A further method used in the work presented is the Voronoi charge analysis.[83] In it the space around the nuclei is divided into polyhedra so that a point in space belongs to the polyhedron of the nearest atom. The electron density of such a polyhedron plus the nuclear charge is the Voronoi charge. As the polyhedra have surfaces in the middle of a bond, the electrons are not divided very sensibly and the Voronoi charges as such are not very useful. The Voronoi deformation density, the difference in Voronoi charges between the fragments of a molecule and the whole molecule, often gives a description in close agreement with e.g. Hirshfeld charges.

A useful tool for looking at the electron distribution in a molecule is the electron localization function (ELF) developed by Becke and Edgecombe.[84,85] A plot of the ELF reveals regions with highly localized electrons, as in covalent bonds or lone pairs.

Another point of great interest to the computational chemist, is what holds the fragments of a molecule together. Several such bond-analysis tools exist. In this work we used the method by Ziegler and Rauk[86] which was later improved by Baerends[87] and which is available in the ADF programme suite.

In the Ziegler-Rauk scheme the bond formation is done in three steps:

1. Bring the fragment from infinite distance to final position, i.e. form a superposition of $\rho_A + \rho_B$ (ΔE= $\Delta \mathrm{V}_{elstat}$)
2. Combine ρ_A and ρ_B to a wave function for the molecule, allowing only for Pauli-relaxation. (ΔE= $\Delta \mathrm{E}_{Pauli}$=$\Delta \mathrm{V}_{Pauli} + \Delta T^0$)
3. Relaxation of the system to its final ground state. This step involves mixing of orbitals. (ΔE= $\Delta \mathrm{E}_{orbital-interaction}$)

Steps 1 and 2 are sometimes combined to a term called 'steric interaction'. The first step, the overlapping of two charge clouds, is always negative in energy. The second step always positive. There is some debate as to what the involved steps mean in the formation of a bond.

2.5.4 Molecular Interactions and the Basis-Set Superposition Error

The interaction potential between two molecules can be split into different contributions[88]

$$V_{int} = V_{elstat} + V_{ind} + V_{disp} + V_{short} \tag{2.108}$$

The first part, the electrostatic part, stems from the interaction of the permanent charge distributions of the molecules. It can be written as

$$V_{elstat} = \frac{1}{4\pi\epsilon_0} \int \rho_a(\mathbf{r}_a) \frac{1}{r_{ab}} \rho_b(\mathbf{r}_b) d\mathbf{r}_a d\mathbf{r}_b \tag{2.109}$$

If the distance between the molecules is big enough, a multipole expansion can be used. In the multipole expansion the electrostatic interaction can be written as:

$$V_{elstat} = Tq^{(a)}q^{(b)} + T_\alpha(q^{(a)}\mu_\alpha^{(b)} + q^{(b)}\mu_\alpha^{(a)}) \tag{2.110}$$

were the T tensors are successive derivatives of the form:

$$T = (4\pi\epsilon_0)^{-1} r^{-1} \tag{2.111}$$
$$T_\alpha = -(4\pi\epsilon_0)^{-1} r_\alpha r^{-3} \tag{2.112}$$
$$T_{\alpha\beta\ldots\nu} = (4\pi\epsilon_0)^{-1} \nabla_\alpha \nabla_\beta \ldots \nabla_\nu r^{-1} \tag{2.113}$$

Here the Einstein notation is used, in which Greek indices mean summation over all cartesian coordinates. The first formula given for the electrostatic interaction is independent of the origo. This is in principle also true for the multipole expansion, but only if it is taken to infinity. If the expansion is truncated, origin dependence is introduced.

The induction energy between two molecules is always negative. It comes from the interaction of the permanent charge distribution of one molecule with the induced change of the charge distribution of the other molecule. For long enough distances, a multipole expansion can be used again. The leading terms of the expansion energy are

$$V_{ind} = -\frac{1}{2}\alpha_{\alpha\beta}^{(a)} F_\alpha^{(b)} F_\beta^{(b)} - \frac{1}{2}\alpha_{\alpha\beta}^{(b)} F_\alpha^{(a)} F_\beta^{(a)} \ldots \tag{2.114}$$

Here $F_\alpha^{(b)}$ is the electric field from molecule b at the point of molecule a and $\alpha_{\alpha\beta}^{(a)}$ are the components of the static-polarisability tensor of molecule a. Induction effects are often quite small compared to electrostatic and dispersion effects.

The dispersion interaction is more difficult to understand. Between two spherical atoms it can be written as the following sum:

$$V_{disp} = \sum_{n=6}^{\infty} C_n r^{-n} \tag{2.115}$$

This equation can in fact be generalised for arbitrary molecules. Often only the leading order term is considered. For long range interactions, the coefficient C_6 can be described by the Casimir-Polder formula.

$$C_6 = \frac{3}{\pi} \int_0^\infty \alpha^A(E)\alpha^B(E) dE \tag{2.116}$$

As noted earlier, dispersion type interactions cannot be described well with DFT methods. For systems were such interactions are important other methods, e.g. MP2 have to be used.

Finally there are the short-range terms. This is a repulsion of the electron clouds of the two monomers at close distance. As the orbitals decay exponentially, this interaction is short ranged and can be described by an exponential function

$$V_{short} = A\exp(-bR) \tag{2.117}$$

These formulas can be used to understand the leading terms in the interaction of two molecules. First, one calculates the energy of a system containing both molecules (the supermolecule) at different distances. From this the energy of the monomers is subtracted. The resulting potential curve represents the interaction potential V_{int}, from it the leading terms can be subtracted.

The problem with this so called supermolecular approach is the basis-set superposition error. In the supermolecule, the basis set of monomer a is partly used to describe monomer b and vice versa. To avoid this problem, the counterpoise correction can be used.[89] At each point of the potential curve, the energy of the fragments is calculated, with the basis set of the other fragment (ghost orbitals) at the appropriate position. This procedure reduces the BSSE but at a high computational cost.

2.6 Software Used

The results presented in this thesis were produced using the techniques described above. These methods are implemented in a number of codes, all with special features, advantages and drawbacks. A short list of the programmes used follows. The programmes are listed alphabetically.

- Amsterdam Density Functional (ADF): ADF is one of the few codes that uses STO basis sets. Integration is done numerically. As the name suggests, it performs density functional calculations. Hybrid functionals present a problem due to the usage of STO's, this has been circumvented recently and new versions of ADF can do a posteriori energy calculations using hybrid functionals. One of the advantages of ADF is that it has basis sets of different quality for all elements of the periodic table, even transactinides. Relativistic effects are included via ZORA, spin-orbit ground state energy calculations can be done. An interesting feature of ADF is the possibility to do energy decomposition analysis of molecular fragments. ADF was used frequently in this work.
- Dalton:[90] Dalton is a free code. It is most useful for the calculation of numerous properties using response theory up to cubic response.
- DIRAC: DIRAC is Dalton's relativistic brother. It can do four-component Hartree-Fock or DFT calculations, MP2 and CC modules also exist. A very nice feature of DIRAC is, that the influence of relativity can be examined by using the complete Dirac-Coulomb Hamiltonian, the spin-free Hamiltonian or the non-relativistic Lévy-Leblond Hamiltonian. It was used for all four-component calculations presented in this work.
- GAMESS-US:[91] This is also a freely available code. A lot of computational methods are available. It was used to calculate anharmonic corrections to vibrational frequencies.
- Gaussian:[92] Probably the most widely used programme in computational chemistry. It can do almost everything but as always in computational chemistry, it is not a black box. It was used to calculate CCSD(T) energies and to perform some geometry optimisations and NBO analysis.
- TURBOMOLE: One of the fastest and most efficient programmes available to do HF, DFT, MP2 and CC2 calculations. Frequencies and electronic excitation energies are also available. Most of the computations presented here were done with TURBOMOLE.

A lot of people have contributed to the field of computational chemistry by providing programmes that facilitate the analysis and interpretation of the results of a calculation. The programmes used here are (in alphabetical order): DGrid,[93] g-Openmol,[94] Ghemical,[95] Molden,[96] Molekel[97] and Xmakemol.[98] All these programmes are freely available. I would like to thank the programmers for their effort.

Chapter 3

Results

The theoretical methods outlined in the previous chapter have been applied to a variety of systems containing heavy metals. The results could be used to explain the bonding in some compounds, to explain interesting properties and in other cases to predict new molecules as viable goals for synthetic chemists. Those results will be presented in the following. Where possible, the published material has been supplemented with previously unpublished results.

3.1 High Oxidation States of Mercury

In compounds, the common oxidation states of mercury are +I or +II. In these states mercury employs its 6s electrons to form bonds. Higher oxidation states would need to employ the 5d electrons as well. As a first evidence of this possibility, Kaupp et al. found that the reaction $HgF_2 + F_2 \rightarrow HgF_4$ is exothermic.[99] More than 10 years after this prediction, the tetrafluoride has still not been made.[100] As a new target for rare-gas matrix studies we calculated HgH_4 and even the hexahydride HgH_6. This may seem energetically a disadvantage. The better hybridization of the smaller hydrogen s- orbital with the mercury 5d-orbitals might overcompensate this disadvantage.

HgH_4 and HgH_6 were calculated in the quadratic planar (D_{4h}) and octahedral (O_h) symmetry, respectively. The optimised bond length decreases slightly when going to higher oxidation states, see Table 3.1. While all the calculated hydrides are exothermic compared with Hg and H_2, they are all energetically far below the atoms.

The transition states for the H_2 loss reaction for the tetra- and hexahydride were found to be of C_2v symmetry. For the tetrahydride the transition state lies 40 kJ/mol above the minimum. For the hexahydride this value decreases to 30 kJ/mol. A trigonal prismatic structure of HgH_6 was also calculated, it lies energetically above the octahedral one and is a transition state with three short H–H contacts. The depth of the potential wells and the ease with which hydrogen atoms can be created in a rare-gas matrix seem to make the hydrides good candidates for synthesizable high-valent mercury compounds. Tunneling may lead to a fast decay of the hydrides, this could be slowed down by using deuterium instead of hydrogen.

The bonding in the tetra- and hexahydrides is easy to understand. The HOMO is a bonding

System	$r_{\mathrm{Hg-H}}$	ΔE
HgH_2	164.5	115.7
HgH_4	163.5	339.7
HgH_6	163.5	575.3

Table 3.1: Bond distances (in pm) and formation energies (in kJ/mol) for mercury hydrides at the CCSD(T) level. The formation energies are zero-point energy corrected for the reaction $Hg(g) + nH_2 \rightarrow HgH_{2n}$.

6p+1s interaction (e_u for the tetrahydride and t_{1u} for the hexahydride). This is followed by a weakly antibonding a_{1g} orbital. Three nonbonding d orbitals follow, they are partly degenerated (e_g+b_{2g}) for the tetrahydride and completely degenerated (t_{2g}) for the hexahydride. The two lowest bonding orbitals are 5d+1s combinations an a_{1g} and b_{1g} for the tetrahydride and an e_g for the octahedral hexahydride.

3.2 On the Short Pt-Tl Bond in $[R_5Pt\text{-}TlR_n]^{n-}$ $(n = 0 - 3)$

In recent years there has been a growing interest in compounds with bonds between transition metals (TM) and main group elements. Special attention has been paid to Group 13 elements.[101,102] There is e.g. a rich boron-transition metal chemistry.[103,104,105] The higher homologues have come under closer scrutiny after the synthesis of compounds with iron gallium-bonds.[106] The bond order was fiercely discussed (see e.g. 107,108). This debate also led to a series of theoretical investigations by Frenking et al.[109,110,111,112,113] He considered for example the bonding in carbonyl complexes of chromium, molybdenum, tungsten and iron with a Group 13 ligand. It was found, that the metal-metal bond is approximately half ionic and half covalent. The covalent part consisted of a σ donation to the TM and a much weaker π back-donation from the TM. The importance of back-donation varied with the substituent on the Group-13 element. Also chromium, molybdenum and tungsten carbonyl complexes with one phosphine ligand were considered. Here a more ionic bond with only a small π character was found.

Another type of compounds, with bonds between a TM and a Group-13 element, are homoleptic compounds with more than one Group-13 ligand. Compounds of the type $(TM)(InR)_4$ are known for nickel[114] and platinum.[115] The Pt-In bond length of 244.1 pm is remarkably short. Such homoleptic compounds are also known for boron, aluminum and gallium, but, to our knowledge, not for thallium. For compounds of this type, the covalent character of the bond is rather large.

Against this general background, it is not surprising to find the series of anions of the general type $[(NC)_5Pt\text{-}Tl(CN)_n]^{n-}$ $(n = 0 - 3)$, **1** - **4**, occurring in compounds recently synthesised by Glaser's group (with sodium as a counterion), with Pt-Tl bond lengths around 260 pm.[116,117,118,119,120] This series has recently been expanded by the synthesis of Pt-Tl compounds with phenantroline ligands around thallium[121] yielding again M-M' bonds of about 264 pm. Such a bond length is, however, very short compared to the earlier Pt-Tl bonds in e.g. $[Tl_2Pt(NC)_4]$, whose experimental x-ray and calculated free-molecule values are 314 and 287 pm, respectively.[122] The difference between the free-molecule and crystal values was attributed to $Tl\cdots(NC)$ interactions in the solid. The compounds **1** - **4** were theoretically studied by Autschbach and Ziegler[123] and by Russo and Kaltsoyannis[124] using density functional theory.

The article on the Pt-Tl bonding situation in the hydride models $[H_5Pt\text{-}TlH_n]^{n-}$ $(n = 0 - 2)$ is included as Paper II in this thesis. Evidence for some $\sigma^2\pi^4$ multiple-bond character was found for these models. We now present as supplementary information a study of the full cyanide systems **1** - **4** and their isoelectronic neighbourhood.

3.2.1 Results for the Cyanide Systems

Structures The results from HF, MP2, B3LYP and BPVWN calculations on **2** are rather similar, see Table 3.2. We carry out the comparison between the various systems at BPVWN level.

Solid **1** exhibits an infinite chain structure $[\text{-}NC\text{-}Pt\text{-}Tl\text{-}]_\infty$. It is therefore not surprising, that the calculated molecular Pt-Tl distance of 317 pm is much above the experimental result 263 pm. Russo and Kaltsoyannis[124] could come down to 260 pm by surrounding the $[(NC)_5Pt\text{-}Tl]$ molecule with water molecules. As an alternative we considered a $[(NC)_5Pt\text{-}Tl\text{-}(NC)\text{-}Pt(NC)_4\text{-}Tl]$ dimer model, whose inner Pt-Tl bond was shortened to 284 pm. Further shortening could be brought about by placing NC^- isocyanides around this central part to simulate crystal effects. The compounds **2** - **4** contain isolated anions. The calculated Pt-Tl distances in Table 3.2 are close to the experimental values, as found earlier by Russo and Kaltsoyannis using the same method.

The vibrational frequencies for the Pt-Tl stretch are also given in Table 3.2. As found earlier, these frequencies are in good agreement with experiment for **2** - **4**, where the comparison is meaningful.

System	Symmetry	Method	R(Pt-Tl)	ν(Pt-Tl)	α(Tl-Pt-C_{eq})
1	C_{4v}	BPVWN	317	51	82.6
		exp.[a]	263	160	-
2	C_{4v}	HF	268	140	88.1
		MP2	255	173	88.2
		B3LYP	268	123	87.6
		BPVWN	271	115	87.5
		exp.[b]	260	161	-
3	C_{2v}	BPVWN	272	133	88.7
		exp.[b]	262	157	-
4	C_1	BPVWN	279	132	91.6
		exp.[b]	264	157	-

[a] Solid state IR and crystal structure data.[117]
[b] EXAFS and aqueous solution IR data.[116]

Table 3.2: Calculated structures and Pt-Tl stretching frequencies for the systems $[(NC)_5Pt\text{-}Tl(CN)_n]^{n-}$, n=0-3, **1** - **4**. Distances in pm, angles in degrees and frequencies in cm^{-1}.

HF	MP2	B3LYP	BPVWN	BPVWN[a]
1.18	1.72	1.15	1.12	1.16

[a] Without counterpoise correction.

Table 3.3: Bond dissociation energy D_e for $[(NC)_5Pt\text{-}Tl(CN)]^-$ into $[(NC)_5Pt]^-$ and TlCN, calculated with different methods. All values in eV.

All calculated frequencies were real.

The chemical binding energies between the $[(NC)_5Pt]^-$ and Tl(CN) moieties, to form **2** are shown in Table 3.3. They are not very large, despite the short Pt-Tl bond length.

Bonding analysis. The various contributions to the Pt-Tl bond between rigid fragments are shown in Table 3.4. In **1**, at R(Pt-Tl)=317 pm, the (CP-uncorrected) bond energy is approximately two third electrostatic and one third covalent. Of the latter 31% comes from a π type interaction. The Pauli repulsion in this system is smaller in size than the electrostatic attraction. Passing from **1** to **2** (R(Pt-Tl)=271 pm), the electrostatic attraction is slightly increased and the orbital attraction is more than doubled in size, but the Pauli repulsion increases by an order of magnitude. Of the total dissociation energy of **2**, 0.245 eV comes from π-type interactions.

In **3** and **4**, the Tl side consists of $Tl(CN)_2^-$ and $Tl(CN)_3^{2-}$ fragments, and these are bound to $(NC)_5Pt^-$. Nevertheless, this global repulsion is more than compensated for by the electrostatic interactions between 'stiff' electron distributions of the fragments, to give an attractive electrostatic interaction of -2.38 and -1.68 eV respectively. We attribute much of this to the interaction between the thallium lone pair and the positive platinum core. The big increase in the Pauli repulsion leads to a rather weak total bonding interaction of -0.22 eV for **3** and a positive value of 0.26 for **4**. This does not mean however, that **4** is not stable. In solution or in a crystal, the negative charge of the molecule would be distributed to surrounding molecules, increasing the stability of **4**.

Electron densities and ELF. A density difference plot between **2** and its fragments is shown in Figure 3.1. Note the increase (light color) between the Pt and Tl atoms. Another interesting feature is the increase of electron density on one side of the equatorial nitrogens. This area of increased electron density is electrostatically attracted to the positively charged Tl atom of the Tl(CN) group. These electrostatic and orbital interactions bend the equatorial CN groups towards Tl in **2**. For **3** such a bending can also be observed. For **4** the opposite is true: the equatorial CN groups bend away from the $Tl(CN)_3^{2-}$ fragment. This is probably so, because the high negative charge of the $Tl(CN)_3^{2-}$ repels the CN groups.

The ELF plot of TlCN (Figure 3.2 left) shows the lone-pair on thallium that is directed towards

	1	**2**	**3**	**4**
Hirshfeld Charges				
q_1	-0.8902	-1.2244	-1.4085	-1.5554
q_2	0.8903	0.2243	-0.5916	-1.4448
Steric Interaction				
Pauli Repulsion	0.6681	4.0902	5.3956	6.5792
Electrostatic Interaction	-2.6051	-3.0271	-2.3838	-1.6771
Total Steric Interaction	-1.9370	1.0632	3.0118	4.9021
Orbital Interactions				
a_1	-0.6357	-1.9557	-3.1075[a]	-4.6403[b]
a_2	-0.0048	-0.0016	-0.0033	
b_1	-0.0066	-0.0186	-0.0665	
b_2	-0.0409	-0.0030	-0.0509	
e_1	-0.3066	-0.2450		
Total Orbital Interaction	-0.9946	-2.2238	-3.2282	-4.6403
Total Bonding Energy	-2.9316	-1.1607	-0.2164	0.2619

[a] For point group C_{2v}. [b] For point group C_1.

Table 3.4: Results of a fragment analysis and Hirshfeld charges of the fragments $[(NC)_5Pt]^-$ and $Tl(CN)_n^{1-n}$ (q_1 and q_2, respectively) for the anions $[(NC)_5Pt\text{-}Tl(CN)_n]^{n-}$ (n=0-3) (**1-4**). All energies are in eV. The calculations were done with the BPVWN functional.

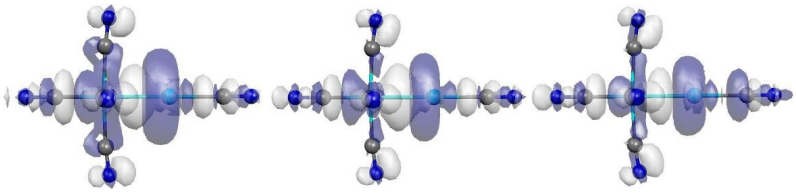

Figure 3.1: Density difference between $[(NC)_5Pt\text{-}TlCN]^-$ and the fragments $(NC)_5Pt^-$ and TlCN. An increase in electron density in the molecule is denoted by light colours, a decrease by dark colours. Calculated at the HF (left), B3LYP (middle) and BPVWN (right) level of theory.

$(NC)_5Pt^-$. The ELF plot of $(NC)_5Pt^-$ (Figure 3.2 right) shows an area of low electron density at platinum directed towards TlCN. As discussed earlier, this makes the two fragments a good fit, and leads to the rather short bond.

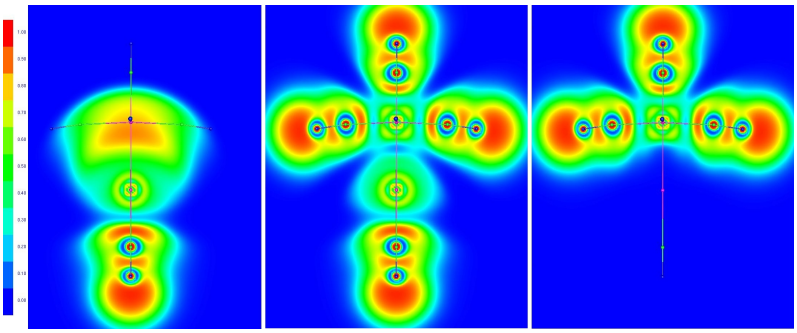

Figure 3.2: Plot of the electron localization function (ELF) of TlCN (left), $[(NC)_5Pt\text{-}TlCN]^-$ (middle) and $(NC)_5Pt^-$ (right) calculated with ADF and Dgrid.

Compound	R(M-M')	R(M'-C)	α(C-M-M')	α(M-C-N)	ν(M-M')
$[(NC)_5Ir\text{-}In(CN)]^{2-}$ (**5**)	264	238	88.1	174.7	129.66
$[(NC)_5Ir\text{-}Pb(CN)]^{-}$ (**6**)	303	247	75.3	149.1	70.09
$[(NC)_5Ir\text{-}Tl(CN)]^{2-}$ (**7**)	270	244	88.1	175.0	106.67
$[(NC)_5Pd\text{-}In(CN)]^{-}$ (**8**)	261	227	86.4	173.4	142.88
$[(NC)_5Pd\text{-}Pb(CN)]$ (**9**)	297	236	79.8	152.9	79.92
$[(NC)_5Pd\text{-}Tl(CN)]^{-}$ (**10**)	272	230	86.6	173.1	122.33
$[(NC)_5Pt\text{-}In(CN)]^{-}$ (**11**)	266	225	87.3	173.8	140.37
$[(NC)_5Pt\text{-}Pb(CN)]$ (**12**)	305	235	79.9	156.9	61.44
$[(NC)_5Pt\text{-}Tl(CN)]^{-}$ (**13**)	271	228	87.5	174.0	115.37

Table 3.5: Calculated structures and M-M' vibrational frequencies for systems isoelectronic to $[(NC)_5Pt\text{-}Tl(CN)]^{-}$. Bond distances in pm, angles in degree and vibrational frequencies in cm^{-1}. All calculations were done with the BPVWN functional.

Isoelectronic systems. A number of valence isoelectronic systems to **2** are shown in Table 3.5. We are using a 5th-row–6th-row substitution or a charge disproportionation such as (Pt-Tl → Ir-Pb) as a guide. The changes in the metal-metal distance are mostly small, suggesting that these alternatives could be viable synthetic objects. The shortest M-M' bond was found in the Pd-In system.

The combination Pd-Pb (**9**) and Pt-Pb (**12**) give longer M-M' bonds. Looking at the Hirshfeld charges in Tables 3.6, 3.7, and 3.8 one notes that the $Pb(CN)^{+}$ moiety in these cases receives electrons from the $M(CN)_5^{-}$ side (M=Pd,Pt), rather than donates them. The π part of the orbital interaction is rather large, which is a hint, that a very effective π back donation from the transition metal shifts electrons to lead. The equatorial cyanide groups bend more towards lead, than to the other metals.

Other ligands. We also calculated the systems $[L_5Pt\text{-}TlL]^{-}$ with L=-F,-Cl,-NC (**2a** - **2c**), as well as $[(NC)\text{-}Pt(NNN)_4\text{-}TlCN]^{-}$ (**2d**). Furthermore the case L=H was studied before.[125] That case lead to even stronger π-type M-M' bonding than any of the present choices. Compared with L=-CN (**2**), L=-Cl gave a comparable R(Pt-Tl), while L=-F,-NC gave slightly longer ones. In **2d**, the azides are strongly attracted by the Tl side. This hypothetical system has a rather unusual, compact structure, in which the N_3 ligands form a bridge between the metals.

Metallophilic attractions are known to arise through dispersion-type mechanisms.[126] A rough measure for them is the shortening of bonds from HF or DFT to MP2 (or higher explicitly correlated levels). We here note such a shortening for **2** in Table 3.2. As mentioned earlier, this may be a sign of some 'metallophilic' character.

3.2.2 Conclusions

1. The short M-M' bonds of system **2** could be reproduced by all methods used,including even HF. No further ligands, such as water, were needed for systems **2** - **4**.

2. The bond energies in a fragment analysis have three comparable components: Attractive electrostatic and orbital interactions and a repulsive Pauli interaction.

3. For **1** - **2** and **5** - **12** well-defined π-type orbital interactions could be identified. In these cases the M-M' interaction could be characterised as a $\sigma^2\pi^4$ triple bond with further electrostatic attraction. These π contributions, however, are smaller than the σ contributions in the present systems.

4. Qualitatively, the σ part consists of a donation from the Tl lone pair to a hole at PtL_5^{-}. The π part consists of a back donation from the latter to the Tl 6pπ orbitals. This picture is not unlike that given earlier by Frenking et al.[110] or Schwerdtfeger et al.[127]

5. The picture of the metal-metal bond we develop explains in a natural way the observed oxidation states between Pt^{IV}-Tl^{I} and Pt^{II}-Tl^{III}.

	$[(NC)_5Ir\text{-}In(CN)]^{2-}$	$[(NC)_5Ir\text{-}Pb(CN)]^{-}$	$[(NC)_5Ir\text{-}Tl(CN)]^{2-}$
Hirshfeld Charges			
q_1	-2.0211	-1.7188	-2.0148
q_2	0.0210	0.7188	0.0147
Steric Interaction			
Pauli Repulsion	4.6044	2.6957	3.4856
Electrostatic Interaction	-4.2081	-8.0101	-3.3227
Total Steric Interaction	0.3963	-5.3144	0.1628
Orbital Interactions			
a_1	-1.3827	-0.9892	-1.1326
a_2	-0.0021	-0.0121	-0.0021
b_1	-0.0157	-0.0879	-0.0194
b_2	-0.0042	-0.0146	-0.0058
e_1	-0.4532	-1.3901	-0.3998
Total Orbital Interaction	-1.8578	-2.4939	-1.5598
Total Bonding Energy	-1.4615	-7.8083	-1.3970

Table 3.6: Results of a fragment analysis and Hirshfeld charges of the fragments for systems, isoelectronic to $[(NC)_5Pt\text{-}Tl(CN)]^{-}$. The fragments were taken to be $[(NC)_5M]^{x-}$ and $M'(CN)^{x+}$. All energies are in eV. The calculations were done with the BPVWN functional.

	$[(NC)_5Pd\text{-}In(CN)]^{-}$	$[(NC)_5Pd\text{-}Pb(CN)]$	$[(NC)_5Pd\text{-}Tl(CN)]^{-}$
Hirshfeld Charges			
q_1	-1.2275	-0.8559	-1.2031
q_2	0.2274	0.8559	0.2030
Steric Interaction			
Pauli Repulsion	4.7132	1.9185	3.3237
Electrostatic Interaction	-3.6373	-4.0156	-2.5422
Total Steric Interaction	1.0759	-2.0970	0.7815
Orbital Interactions			
a_1	-2.0292	-0.7470	-1.5305
a_2	-0.0018	-0.0081	-0.0014
b_1	-0.0196	-0.0864	-0.0204
b_2	-0.0024	-0.0090	-0.0032
e_1	-0.3186	-0.9397	-0.2565
Total Orbital Interaction	-2.3715	-1.7902	-1.8120
Total Bonding Energy	-1.2956	-3.8872	-1.0305

Table 3.7: Results of a fragment analysis and Hirshfeld charges of the fragments for compounds isoelectronic to $[(NC)_5Pt\text{-}Tl(CN)]^{-}$. The fragments were taken to be $[(NC)_5M]^{x-}$ and $M'(CN)^{x+}$. All energies are in eV. The calculations were done with the BPVWN functional.

	$[(NC)_5Pt\text{-}In(CN)]^-$	$[(NC)_5Pt\text{-}Pb(CN)]$	$[(NC)_5Pt\text{-}Tl(CN)]^-$
Hirshfeld Charges			
q_1	-1.2494	-0.8709	-1.2244
q_2	0.2493	0.8710	0.2243
Steric Interaction			
Pauli Repulsion	5.1783	1.7386	4.0902
Electrostatic Interaction	-3.9188	-3.7112	-3.0271
Total Steric Interaction	1.2595	-1.9725	1.0632
Orbital Interactions			
a_1	-2.3454	-0.7814	-1.9557
a_2	-0.0017	-0.0076	-0.0016
b_1	-0.0153	-0.0685	-0.0186
b_2	-0.0016	-0.0085	-0.0030
e_1	-0.2662	-0.7867	-0.2450
Total Orbital Interaction	-2.6302	-1.6526	-2.2238
Total Bonding Energy	-1.3707	-3.6251	-1.1607

Table 3.8: Results of a fragment analysis and Hirshfeld charges of the fragments for compounds isoelectronic to $[(NC)_5Pt\text{-}Tl(CN)]^-$. The fragments were taken to be $[(NC)_5M]^{x-}$ and $M'(CN)^{x+}$. All energies are in eV. The calculations were done with the BPVWN functional.

6. A number of possible chemical extensions of the systems synthesised by Glaser et al. were explored.

3.3 Bonding in U(VI) Systems

Actinide chemistry is a very interesting area. For the early actinides many different oxidation states are possible and in aqueous solution they might even be present at the same time. The redox chemistry of Pu is one of the most complex in the whole periodic table. Computationally the actinides are very challenging as relativistic effects become very important. In addition systems containing actinides not in their highest oxidation state, are often multi-configuration systems and therefore difficult to treat. For the heavier, highly radioactive, actinides experimental data is scarce.

For uranium experimental data is abundant, but its chemistry is still full of surprises. It is for example striking, that while uranium halides are numerous, uranium cyanides are very rare. In the few examples known, the uranium actually binds to the nitrogen end. Usually pseudohalogens are very similar to halogens, hence their name.

The bonding situation is already quite interesting in the much studied UF_6. It has 36 valence electrons forming an

$$e_g^4 + t_{2g}^6 + 1t_{1u}^6 + a_{1g}^2 + t_{2u}^6 + t_{1g}^6 + 2t_{1u}^6 \tag{3.1}$$

orbital structure (in O_h symmetry). With the 2pσ orbitals fluorine can form six single bonds, but there is also a back donation from the 2pπ orbitals of fluorine to uranium 5f and 6d orbitals. All in all the orbital structure above can be split into 6 σ bonding, 6 π bonding, three nonbonding and three antibonding orbitals. This gives a theoretical bond order of 1.5 for the U-F bond. This could not happen for transition metal fluorides, as the bonding to the f orbital is necessary for the higher bond order. Both NBO and fragment analysis show the π contribution. A further proof is the bond length of UH_6. The difference in bondlengths between UH_6 and UF_6 is 6 pm, the difference in covalent radii

is 34 pm. The hydride simulates a fluoride without π bonding, the shortening of the U-F bond can then be explained as a π contribution.

The explanation for the remarkably strong bond is that the uranium atom is a good σ donor, while the fluorine atom is a good σ acceptor. After formation of the σ bonds, uranium is a good π acceptor and fluorine a good π donor. The two are a perfect match. The bond is further strengthened by ionic contributions. The cyanide on the other hand is a good σ donor and π acceptor and hence unfit for bonding to U(VI). As the nitrogen end of cyanide is a better π donor, in the few uranium cyanide compounds known, the uranium bonds to the nitrogen.

The same reasoning used for fluorine can be used for oxygen in $U(OX)_6$ compounds. This then explains the well known oxophilicity of uranium.

We calculated a number of compounds of the type UF_4X_2, where X is a halogen or pseudohalogen. Reaction energies, vibrational frequencies and fragment analysis supported our picture. The U-F bond is strongest, -NC is more strongly bonded than -CN and the triatomic pseudohalogens form stronger bonds than the two-atomic ones.

The triatomic pseudohalogens are more polarisable, especially the isothiocyanate. They can transfer electron density to the atom bonded to uranium and hence improve its π donor quality. This explains, why three-atomic pseudohalogen complexes of U(VI) are more numerous.

As mentioned above, a number of uranium halides is known experimentally. For fluorine and chlorine U(III) to U(VI) halides exist. For the heavier halogens the number of systems with a high oxidation state of uranium is much smaller. Especially U(VI) systems with iodine bonds have until recently been unknown.[128] Therefore we extended our analysis of U(VI) systems to include all halides and the mixed halides UF_4X_2 up to iodine. These new results are presented here.

The same techniques were used as described in Paper III included in this thesis. The frozen core approach was used and all electrons up to 3p for bromine and 4p for iodine were considered frozen.

We start with the pure halides. Geometrical data and results for different population analysis methods are given in Table 3.9.

	U in UF_6	U in UCl_6	U in UBr_6	U in UI_6
r_{U-X}	202.53	247.16	263.64	286.88
Mulliken	2.5978	1.0706	1.9653	0.3876
Hirshfeld	0.9793	0.4618	0.3734	0.2407
Voronoi	0.4980	0.4500	0.4330	0.3200

Table 3.9: Bond lengths and atomic charges for uranium in UX_6 systems. The bond lengths are given in pm.

Voronoi and Hirshfeld charges agree quite well, the Mulliken charges are somewhat off. Note, that the Mulliken charges do not follow the trend of higher charges when going to lighter halogen and that the Voronoi charge for UF_6 is rather low.

The results of a fragment analysis of the UX_6 systems are given in Table 3.10. One should be aware, that if done like this, the analysis also contains X-X interactions. The electrostatic interaction is bigger for the heavier halogens, as the more diffuse charge cloud of the heavier halogens overlap more than those of fluorine, but the difference is rather small.

The biggest difference lies in the orbital interactions. Fluorine has almost twice as big orbital interactions as iodine. The orbital-interactions are a bit difficult to resolve, as X-X interactions might appear here as well. Note, that the t_{2u} and t_{2g} interactions decrease sharply for the heavier halogens. These interactions arise from π backbonding of the ligand. The heavier halogens are increasingly bad π donors. The sum of the orbital interactions fall off when going to the heavier halogens. Only the a_{1g} interaction is slightly increased, this interaction might contain X-X contributions. The total bonding energy falls off rapidly from fluorine to chlorine, then the changes become much smaller. The bonding energy of UF_6 is almost twice that for UI_6

As it is impossible to filter out the X-X interactions in the analysis of UX_6 systems, we considered the mixed halides UF_4X_2. This also makes a direct comparison possible with the results for the other

	UF_6	UCl_6	UBr_6	UI_6
r_{U-X}	202.53	247.16	263.64	286.88
Steric Interaction				
Pauli Repulsion	95.8102	83.4906	78.1652	72.1221
Electrostatic Interaction	-26.2139	-29.4827	-30.7887	-30.6764
Total Steric Interaction	69.5963	54.0079	47.3765	41.4457
Orbital Interactions				
a_{1g} (σ)	-4.6227	-5.8528	-5.1505	-5.1349
e_g (σ)	-39.3066	-29.2883	-26.0633	-22.7216
t_{1g} (π)	-11.6381	-8.6367	-7.8689	-6.9598
t_{2g} (π)	-22.8415	-19.1047	-17.1474	-14.8476
a_{1u}	2.3665	2.2846	2.2766	2.1296
t_{2u} (π)	-8.1875	-4.7569	-3.6949	-2.7699
t_{1u} ($\pi + \sigma$)	-28.8056	-19.2319	-16.7954	-14.1902
Total Orbital Interactions	-113.0372	-84.5596	-74.4164	-64.4647
Total Bonding Energy	-43.4410	-30.5517	-27.0400	-23.0190

Table 3.10: Fragment analysis of UX_6 systems. The fragments were the spherically averaged atoms. All energies are given in eV.

ligands given in Paper III. A fragment analysis was performed for trans-UF_4X_2, with UF_4^{2+} and X_2^{2-} as the fragments. The results of this analysis are given in Table 3.11.

	UF_6	UF_4Cl_2	UF_4Br_2	UF_4I_2
r_{U-F}	202.5	202.1	201.9	202.0
r_{U-X}	202.5	250.6	265.6	289.1
Steric Interaction				
Pauli Repulsion	16.0725	12.0424	10.4593	8.7738
Electrostatic Interaction	-33.5916	-26.3547	-25.8242	-22.9085
Total Steric Interaction	-17.5192	-14.3122	-15.3649	-14.1348
Orbital Interactions				
a_{1g} $(\sigma)^c$	-1.9395	-2.3666	-2.7004	-2.8533
a_{2g}	-0.0222	-0.0152	-0.0120	-0.0097
b_{1g}	-0.0598	-0.0395	-0.0301	-0.0251
b_{2g} (π)	-0.0506	-0.0327	-0.0248	-0.0205
e_{1g} (π)	-2.0091	-1.8856	-1.9630	-1.7652
a_{1u}	0.0000	0.0000	0.0000	0.0000
a_{2u} (σ+π)	-3.5231	-2.7018	-2.8182	-2.8445
b_{1u}	0.0000	0.0000	-0.0001	-0.0015
b_{2u} (π)	-0.1835	-0.1201	-0.0904	-0.0764
e_{1u} (π and σ+π)	-3.2359	-3.0682	-3.3045	-3.5380
Total Orbital Interactions	-11.0236	-10.2296	-10.9436	-11.1342
Total Bonding Energy	-28.5428	-24.5418	-26.3086	-25.2689

Table 3.11: Fragment analysis of UF_4X_2 systems. The fragments were taken as UF_4^{2+} and X_2^{2-}. Bond distances are given in pm and energies in eV.

The U-X bonds in the mixed halides are very close to the ones in the pure halides. In the fragment analysis UF_4Cl_2, UF_4Br_2 and UF_4I_2 are remarkably similar. Iodine and bromine make a weaker bond than fluorine but a bit stronger than chlorine. Pure σ-bonding is stronger and π-bonding is weaker for Cl, Br and I as compared to F. The rising a_{1g} contributions are partly due to interactions of the X_2^{2-} with the fluorines of the UF_4^{2+}, but this contribution will be much smaller than for the UX_6 systems.

Note, that the electrostatic interaction decreases from F to I for UF_4X_2 systems. It was increasing for UX_6 systems. This is a clear indication of stronger X-X interactions in UX_6 when going to heavier halogens.

The pure halides of iodine and bromine may be difficult to synthesise, as bonding is much weaker. But for mixed systems the chances are much better. The first system with a U(VI)-I bond to be synthesised was $UO_2I_4^{2-}$.[128]

3.4 Similarities in the Periodic Table, $[Au{=}C{=}Au]^{2+}$ and Related Systems

Similarities in the periodic table are often interesting and can lead to new insights into the chemical properties of the elements involved. The very low melting point of mercury has been attributed to relativistic effects, mainly due to the relativistic contraction of the $6s^2$ shell.[129] This lowers the depth of the interatomic potential and hence the strength of the metallic bond. Mercury could be seen as a pseudo rare gas. If that is the case, then gold could be seen as a pseudohalogen, and in fact gold is known to form aurides like CsAu were gold is in the oxidation state -1. Continuing this series, Au^+ or the isoelectronic platinum could be seen as pseudo oxygens (or pseudo chalcogens). We investigated a number of systems in which gold and platinum could be seen as heavy analogues of oxygen. In the systems considered, beautiful multiple bonds to the heavy metals are present.

The chalcogenic behaviour of Au^+ and Pt can be explained by the electronic structure, they have a σ hole ($5d^{10}6s^0$), like oxygen ($2p\sigma^0$). Like oxygen they can act as π donators. The smallest systems studied are the heavy analogues of $C{\equiv}O$, AuC^+ and PtC. Especially AuC^+ has been studied before and a triple bond has been predicted.[130] This system was used to calibrate our methods. The calibration showed, that B3LYP calculations with a TZVPP basis set were the best affordable combination.

The next system we investigated was $[Au{=}C{=}Au]^{2+}$, a heavy analogue of CO_2. Only a linear minimum was found. The singlet state was confirmed to be the lowest. The gold-carbon distance is slightly longer than in AuC^+, confirming our picture of a lower bond order. In the heavy analogue of diethyl ether $Au(CH_3)_2^+$ the gold carbon distance is more than 22 pm larger. Although $[Au{=}C{=}Au]^{2+}$ is not thermodynamically stable with respect to decomposition into Au^+ and CAu^+, the calculated reaction barrier of 1.61 eV is big enough to make it experimentally observable. This supports Gibson's claims of a linear structure for CAu_2^{2+} observed in a mass spectrum.[131] For the isoelectronic Pt=C=Pt we find also a stable singlet ground state and even shorter bond lengths, which can be explained by the missing charge. A rather novel description could be given for platinum carbonyl, it could in principal be seen as a heavy analogue to an 'unsymmetric' CO_2, then it could be written as Pt=C=O.

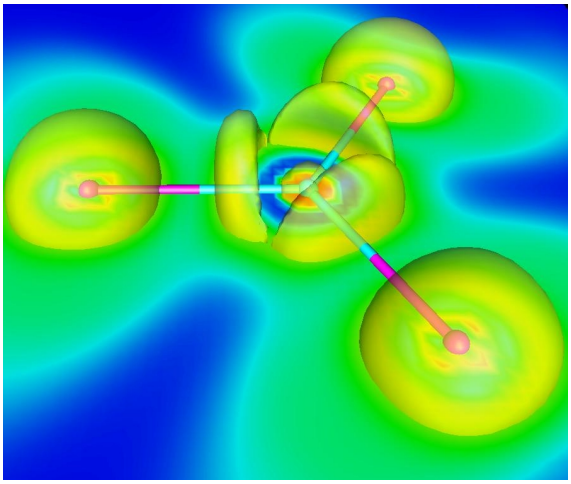

Figure 3.3: Cut plane through the ELF of BAu_3. An isovalue plot of the ELF is superimposed.

Adding one more heavy atom to the system, we arrive at analogues to the carbonate ion CO_3^{2-}. Both CPt_3^{2-} and the isoelectronic CAu_3^+ were studied. Both have minima of D_{3h} symmetry with bond lengths between single and double bonds, matching the bond order of 1.33 found in the carbonate ion. A rather interesting neutral system is BAu_3. Here the MO picture shows four bonding orbitals. For three bonds, this leads to a theoretical bond-order of 1.33 as expected. The electron localisation function (ELF) of BAu_3 in Figure 3.3 reveals disc shaped areas of electron density, typical for multiple bonds.

An interesting case is AuCCAu. It can either be seen as a heavier analogue of acetylene H–C≡C–H or it can, in the spirit of this investigation, be compared to the experimentally known $[O{=}C{=}C{=}O]^{2-}$. The Au–C bond is in fact shorter than a normal single bond supporting the latter analogy.

These systems can be extended by lengthening of the carbon chain, the heavy analogues of carbon suboxide, PtCCCPt and $[AuCCCAu]^{2+}$, were the biggest system investigated in this study. These systems show again strong double bonds between the heavy metals and carbon.

An interesting concept in transition-metal chemistry is Hoffmann's isolobality principle. The d and s orbitals of a transition metal in a complex can be compared to simple first row fragments like methylidene or methylidyne. In the case of methylidyne (≡CH) the following analogies exist:
$\equiv CH \longleftrightarrow M(d^5)L_5 \longleftrightarrow M(d^9)L_3 \longleftrightarrow M(d^{10})[\eta^5(cp)]$
It is interesting to note, that the same lobes as in ≡CH exist in our compounds without the need of ligands at the backside of the transition metal. This behaviour can be called 'autogenic isolobality'.

The presented analogy works very well for the investigated systems. This new idea suggests some interesting candidates for systems with multiple bonds to gold which otherwise are rare.

3.5 Properties of WAu_{12}

Highly symmetrical systems are pleasing to the eye. WAu_{12}, an especially beautiful molecule with high symmetry was predicted recently by Pyykkö and Runeberg.[132] WAu_{12} is a golden icosahedron with a tungsten atom in the middle. With 12 electrons from the gold and the six electrons of tungsten ($5d^46s^2$) it complies with the 18 electron rule. The aurophilic attraction further stabilises the system. Finally relativistic effects are important. This stable molecule was prepared a short time after its prediction from a mixture of the metal vapours.[133] The ease with which it is formed might make it possible to synthesise larger quantities of WAu_{12}.

Little was known about the molecule. In order to better understand the bonding and to aid spectroscopists in the detection of WAu_{12} we conducted a thorough study of its properties.

DFT,MP2 and CC2 geometry optimisations were performed. Due to the importance of the metallophilic attraction, a dispersion interaction badly described by DFT-methods, the MP2 and CC2 bond lengths are much shorter. MP2 often overestimates these effects and the true bond distance probably lies between the obtained results.

Three highly symmetric structures for WAu_{12} are possible. These are shown in Figure 3.4. The icosahedron was found to be lowest in energy. The pentadecahedron is a transition state for the intramolecular transition from one icosahedral structure to the next (rotating the top half of the icosahedral form in Figure 3.4 by 30° gives the pentadecahedron in the middle). The cubeoctahedron is a minimum on all DFT levels, but a saddle-point for MP2. It lies at least 20 kJ/mol above the icosahedron.

A number of calibration calculations were performed with ADF on WAu_{12} in order to assess the best combination of basis set and functional to be used in the study. The results are given in Table 3.12 to supplement the information in the article. These results show that it is justified to use large frozen cores and TZP basis sets for geometry optimisations and frequency calculations.

The vibrational spectra show a remarkable property of WAu_{12}. At room temperature the intramolecular rotation described above occurs 10^8 times per second. This enormous flexibility might enhance the catalytic activity of WAu_{12}. This property may be compared with the non-existence of frozen interstitial atoms in gold down to 0.3K.[134]

An important part of the examination of WAu_{12} was to understand the bonding. Apart from Mulliken population analysis, which fails completely, all other methods used show a slightly positive

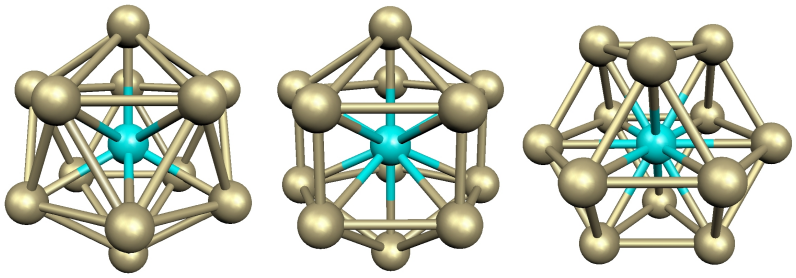

Figure 3.4: The three possible structures of high symmetry of WAu_{12}. The icosahedron (I_h) left is lowest in energy. The pentadecahedron (D_{5h}) in the middle is a transition state. The cubeoctahedron (O_h) right is a local minimum at DFT level, but a saddle-point at MP2.

	BP86	BLYP	PW91	PBE	PBE/SmallCore
DZ					
r(W-Au)	278.73	278.76	278.71	278.72	
E(bond)	-38.133	-36.248	-39.729	-39.379	
TZP					
r(W-Au)	276.15	278.70	275.85	275.57	274.96
E(bond)	-36.165	-34.207	-37.492	-37.208	-37.407
TZPP					
r(W-Au)	274.22	275.37	274.23	273.84	
E(bond)	-37.212	-35.209	-38.551	-38.272	

Table 3.12: Additional calibration calculations for WAu_{12}, performed with ADF.

tungsten.

An old method to analyse the oxidation state of an atom in a molecule is the use of electron spectroscopy for chemical analysis (ESCA).[135] A plot of the oxidation state of an atom against the energy of a lower lying orbital of this atom for different compounds should give a straight line. Measuring the orbital energy of the atom in a new compound, this line can then be used to assign an oxidation state to the atom in question. We used this method in a computational way. To our knowledge, this was done for the first time. The result was an oxidation state of +1.5 for tungsten and +0.7 for gold, supporting the picture of a more positive tungsten.

An interesting way to look at the electron distribution of a molecule is the use of the electron localisation function (ELF). A plot of the ELF is shown in Figure 3.5. This picture was elected as the title picture for the number of Phys Chem Chem Phys in which the article appeared. The ELF shows nicely a buildup of electron density between gold an tungsten, a bond is formed. Another feature of the ELF is a buildup of electron density on the backside of the gold atoms. These electrons could sustain a ring current in WAu_{12}, that might make the molecule aromatic. The formation of a bond was also supported by another method. The electron-density difference between WAu_{12} and its constituent atoms was integrated in spheres of different radii. Here a build-up of electron density between gold and tungsten was found. Writing the formula of WAu_{12} as $W@Au_{12}$ should therefore be avoided.

The electronic excitation spectrum of WAu_{12} was calculated at the TDDFT, CCS and CC2 level of theory. While the spectra look quite different they all show absorption in the visible region between 380 and 460 pm. This would give - not surprisingly - bulk WAu_{12} a pale yellow colour. It should be noted, that CCS fails dramatically, double excitations are of extreme importance, even CC2 might not be sufficient to describe the excitation spectrum correctly.

Finally some magnetic properties were calculated. A striking feature is the very strong shielding of the tungsten nucleus. The spin-orbit coupling contribution is also one of the biggest calculated for a tungsten nucleus. Due to very fast spin flips of the gold system, the tungsten NMR should show one signal. If the spin lattice relaxation is slow but the molecular rotation fast, the signal might split up

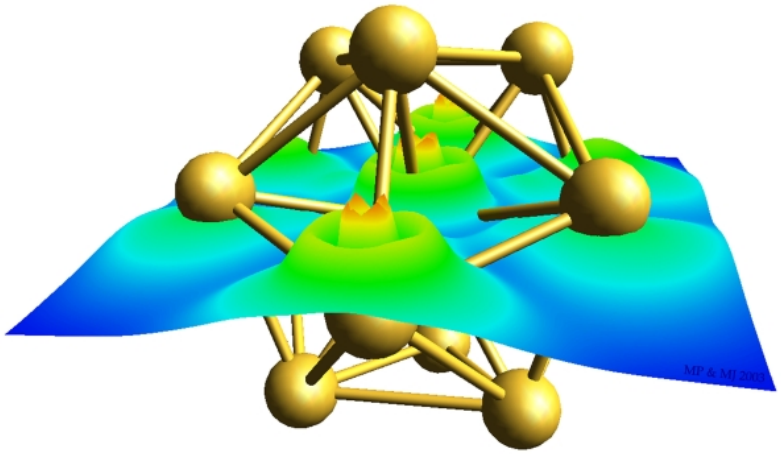

Figure 3.5: A cut through the electron localisation function of WAu_{12} superimposed on its icosahedral structure.

into a weighted trisdekaheptuplet.

WAu_{12} does not only have a beautiful structure but also fascinating properties and one hopes that larger quantities of this compound will indeed be synthesised in the near future.

3.6 The Structure of Mono- and Bis-Gold(I)-Thiocyanate Complexes

The coordination chemistry of gold is rich. Au(I) complexes of the heavy halides and the pseudohalides are known. Recent experiments showed, that such monoaurated halides can be further aurated to give digold(I)halogenium ions.[136] This work was extended to include pseudohalides.[137] Diauration of the thiocyanate ion was achieved in the following reaction

$$(\mathrm{R_3P})\mathrm{AuSCN} + [(\mathrm{R_3P})\mathrm{Au}]^+\,\mathrm{Y}^- \xrightarrow[-78^\circ]{\mathrm{CH_2Cl_2}} \{[(\mathrm{R_3P})\mathrm{Au}]_2\mathrm{SCN}\}^+\,\mathrm{Y}^-. \tag{3.2}$$

where R is Ph, (2-Me-C_6H_4)$_3$, (3-Me-C_6H_4)$_3$, ^{i}Pro$_3$ or Me_2Ph. No x-ray spectroscopy was possible, therefore the structure of the compound is still unknown. The μ^2-S structure is only one possible isomer. Some spectroscopical data could be obtained and we turned our attention to these systems to help in determining the correct structure.

Highly accurate gas phase vibration data exists for the thiocyanate ion.[138] We started our investigation by doing calibration calculations on the thiocyanate ion. These calculations showed that CCSD(T) calculations and anharmonic corrections must be used to get good agreement with experiment. Such high-level calculations are not feasible for the somewhat large diaurated systems. We decided to use MP2 with an admittedly rather small cc-pVDZ basis set augmented by polarisation f-functions[139] on the gold. DFT methods could not be used as they have problems describing the dispersion-type aurophilic interactions correctly. Calculation on the $[(H_3PAu)_2Cl]^+$ ion showed that this basis set with MP2 gave rather good agreement with experiment.

The bulky phosphine ligands increase the computational cost. Calculations on the model H_3PAuSCN and the known Me_3PAuSCN and similar systems showed, that the nature of the group R has no great

influence on the structure and vibrational frequencies. The hydride model was therefore used in this study.

In the experimentally observed monoaurated compounds the gold was always bound to the sulfur of the thiocyanate. This is not surprising as gold is known to be thiophilic. We optimised both the N- and S-bonded structures. While the N-bonded structure has a linear SCN-Au chain, the NCS-Au isomer has an angle of 94.2°. The vibrationally corrected isomerisation energy is surprisingly low, only 15.1 kJ/mol, favouring the S-bonded isomer. This value is in good agreement with an experimental estimate of 18.0 kJ/mol.

Next the diaurated systems were considered. Three different isomers are possible. They are part of the equilibrium

$$\{[(\mathrm{R_3P})\mathrm{Au}]_2\mathrm{SCN}\}^+ \rightleftharpoons \{[(\mathrm{R_3P})\mathrm{Au}]\mathrm{SCN}[\mathrm{Au}(\mathrm{PR_3})]\}^+ \rightleftharpoons \{[(\mathrm{R_3P})\mathrm{Au}]_2\mathrm{NCS}\}^+, \qquad (3.3)$$

The structures of the three isomers were optimised. Some structural results and relative energies are summarised in Table 3.13. Gas-phase MP2 data would indicate that the μ^2-S structure is highest in energy. This is rather surprising and it contradicts the experimental estimate which sees the μ^2-S structure below the μ^1-S μ^1-N structure. The extrapolated C-N stretching frequencies are in good agreement with experimental data. Only the predicted band at 1952 cm^{-1} for the μ^2-N isomer was not observed.

	R(Au–Au)		ΔE_{iso}			
	RHF	MP2	RHF	MP2	MP2[a]	Exp.est.
$[(\mathrm{R_3PAu})\mathrm{SCN}(\mathrm{AuPR_3})]^+$	612.2	583.9	0	0	0	0
$[(\mathrm{R_3PAu})_2\mathrm{NCS}]^+$	377.8	341.4	+39.8	+33.1	+30.1	-
$[(\mathrm{R_3PAu})_2\mathrm{SCN}]^+$	416.5	320.8	+58.6	+44.4	-5.0	≈-8.4

[a] Dielectrical continuum effects of CH_2Cl_2 were considered by using the COSMO model.

Table 3.13: Gold-gold distances [R(Au–Au) in pm] of the three isomeric diaurated thiocyanate cations (with R = H) calculated at the RHF and MP2 level. The isomerisation energies (ΔE_{iso} in kJ/mol) relative to $[(\mathrm{R_3PAu})\mathrm{SCN}(\mathrm{AuPR_3})]^+$ calculated at different levels are also given.

The experiment was carried out in dichloromethane, not in vacuum. We included the effects of the solvent with the COSMO method[140] as implemented in TURBOMOLE. This changed the energetic ordering completely and yielded more believable isomerisation energies with the μ^2-S isomer energetically lowest. The computational method employed could indeed help to assign a structure of the synthesised digold(I)thiocyanate cations.

3.7 A Comparison of Small Molecules Containing Darmstadtium and Platinum

The heaviest element for which calculations are reported here is element 110, darmstadtium. There are only three research centres in the world where new elements are currently being prepared. Not only is it difficult to prepare a few nuclei of the element, one also has to work fast, as all the transactinides are rather shortlived. There is a change in paradigm in the 'super-heavy element' community.[141] It becomes more important to discover the chemistry of the new elements than to produce new heavier elements. Computational chemists can be of some assistance here.

The transactinides made so far have rather short lifetimes and make chemical reactions rather difficult. Certain neutron rich isotopes of Ds were calculated to have a lifetime of up to 50 years, which would make chemical experiments much easier.[142]

The early transactinides resemble their lighter homologues quite closely. For Rg (element 111) and element 112 some changes in properties were reported. The question arises if there is a certain break in similarity (*transactinide break*). If yes, it should occur for element 110, darmstadtium. One difference

between Ds and its lighter homologue Pt is the ground state electron configuration. It changes from $(d_{3/2}d_{5/2})^9s^1$ for platinum to $d^4_{3/2}d^4_{5/2}s^2$ for Ds.[143]

We optimised the geometries for the carbides, carbonyls and the tetra- and hexafluorides of platinum and darmstadtium. The bond distances were found to be very similiar for Ds and Pt. Also the calculated vibrational frequencies agree closely. Spin-orbit coupling does not change the geometry. A fragment analysis of the carbonyls and carbides gives similiar results for Pt and Ds, with slightly larger orbital interactions and Pauli repulsion, leading to slightly weaker bonds for the transactinide.

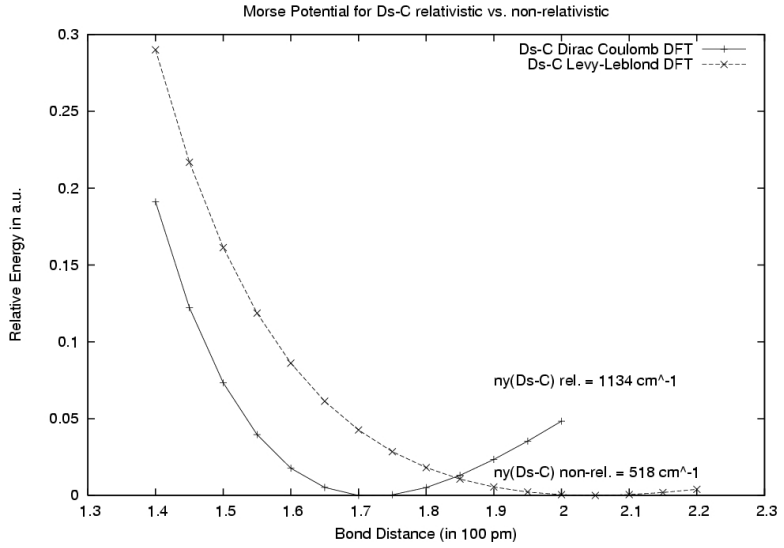

Figure 3.6: The potential curve of DsC calculated relativistically and nonrelativistically.

The extreme importance of relativistic effects for Ds in shown on Figure 3.6. Not only is there a 15.8 % relativistic contraction of the bond length. The potential curve is changed dramatically, leading to a relativistic increase in the vibrational frequency from 518 cm^{-1} to 1134 cm^{-1}, an increase of 119 %.

To test if the calculated Ds compounds have a singlet ground state, we calculated the 30 lowest singlet and triplet excitation energies for the carbide and the carbonyl. The results for the lowest of these are given in Tables 3.14 and 3.15. The excitation energies were calculated at the time dependent DFT level of theory using the LB94 exchange correlation functional with ADF. All electrons were considered active and a basis set of QZ quality was used. The special GGA functional LB94 was designed to give the right asymptotic behaviour and therefore normally gives quite good excitation energies.

Singlet				Triplet		
Symmetry	Degeneracy	Energy	Intensity	Symmetry	Degeneracy	Energy
Φ	2	2.80634	0	Π	2	2.54254
Π	2	3.04282	0.3889E-02	Φ	2	2.56664
Π	2	4.27789	0.1990E-01	Π	2	3.72332

Table 3.14: The lowest singlet and triplet excitation energies for DsC. The energies are given in eV. Two component calculation without spin-orbit coupling, therefore the triplet excitations have no intensities.

One difference between the late transactinides and their lighter homologues was reported for Rg. For the halides, the higher oxidation states of Rg were more stable than for Au. The decomposition reaction $MF_6^- \rightarrow MF_4^- + F_2$ was found by Seth et al. to be more endothermic by 0.89 eV for Rg (B3LYP results).[144] For Ds and Pt we find the same, although the energy difference is smaller, only

Singlet				Triplet		
Symmetry	Degeneracy	Energy	Intensity	Symmetry	Degeneracy	Energy
Δ	2	1.79786	0	Δ	2	1.64066
Φ	2	3.33599	0	Σ_+	1	3.07503
Σ_+	1	3.44322	0.2273E-01	Π	2	3.11461

Table 3.15: The lowest singlet and triplet excitation energies for DsCO. The energies are given in eV. Two component calculation without spin-orbit coupling, therefore the triplet excitations have no intensities.

0.2 eV (PBE results). Part of the difference might originate from the functionals used. Nevertheless, there seems to be a smooth onset of the increased stability of higher oxidation states.

In conclusion, Ds seems to be a normal member of group 10, no *transacinide break* was observed. The work on transactinides has been continued to predict triple-bond radii for these elements.[145]

Chapter 4

Conclusions

Inorganic chemists get more and more skilful in synthesizing interesting new compounds. New and improved spectroscopic methods give deeper inside into the studied molecules. Where is the place for theoretical chemistry? It cannot be the goal of computational chemistry to reproduce experimental numbers. The aim should be to predict new species or to explain aspects of the bonding or certain properties of molecules, that experimentalists cannot access. It is of course important to compare theory and experiment. A good computational work that arrives at different results as compared to an experimental study should make both the experimentalist and the theoretician think again. The development of computers over the last decades has led to an interesting situation. Every researcher nowadays has the computational power at hand to do serious calculations, but is this really necessary? I am a chemist by training, I have worked many hours in laboratories and I liked it. Still, I would not start unguided with a difficult synthesis neither would I try to build spectroscopical equipment. I would trust experienced experimentalists to do this work. Likewise I hope that experimentalists will learn to trust theoreticians. It is the combination of theory and experiment that yields new insights.

Theoreticians can do experiments that would be very dangerous or difficult or even impossible to perform in a laboratory. We can do studies on poisonous and highly radioactive compounds without any danger. We can even change the speed of light *in silico* to get deeper insights into relativistic effects. The research presented here was done with this in mind. In Paper I of this thesis we propose new species with high-valent mercury. Experimentalists are still trying to synthesise these compounds, so more computational work might be needed. In the study on Pt–Tl compounds, presented in Paper II of this thesis, we could explain the experimental observation of the oxidation state for platinum and thallium. Here our calculations delivered data, that experimentalists could not obtain. We were on the other hand able to use the experimental data available to calibrate our calculations.

Experimental chemists have developed an amazing set of simple tools and rules to predict the reactivity of elements and their compounds. Here computational chemistry can contribute by helping to develop new rules in cases were the experimentalists have not gathered enough data, or the theoretician can explain why a certain rule might not work properly. In our study of U(VI) compounds, Paper III of this thesis, we could both give a new picture of the bonding in UF_6 and explain why certain U(VI) compounds are very rare, thus helping to understand this experimental fact. In our research on similarities in the periodic table, Paper V, we found interesting parallels between oxygen and platinum, subsequent studies could in fact expand this to an analogy between iridium and nitrogen.[146] These analogies might prove useful to explain the behaviour of certain transition metals.

A fascinating area of research is the transactinide chemistry. It is extremely expensive to create just a few atoms of those super-heavy elements. Experiments to test the chemical behaviour of these elements have to be thoroughly planned. The more theoretical data the experimentalists have available, the better can they decide what to study. In our research on darmstadtium, Paper VII, we found similarities to platinum. The assumed *transactinide break* was not observed.

This short summary shows how important and fruitful the collaboration of theory and experiment can be. I sincerely hope, that the mutual trust and understanding between experimentalists and theoreticians will grow in the future. If this research helps in accomplishing this, I am satisfied.

References

[1] Pyykkö, P. *Chem. Rev.* **1988,** *88,* 563.

[2] Pyykkö, P. *Lecture Notes in Chemistry, Springer-Verlag, Berlin* **1986,** *41,* 389 pp.

[3] Pyykkö, P.; Kutzelnigg, W. *Lecture Notes in Chemistry, Springer-Verlag, Berlin* **1993,** *60,* 479 pp.

[4] Pyykkö, P. *Lecture Notes in Chemistry, Springer-Verlag, Berlin* **2001,** *76,* 362 pp.

[5] "DATABASE 'RTAM"', Pyykkö, P.; University of Helsinki, Finland, 2005 URL: http://www.csc.fi/rtam/.

[6] Messiah, A. *Quantum Mechanics;* North-Holland: Amsterdam, 1962.

[7] Szabo, A.; Ostlund, N. S. *Modern Quantum Chemistry;* Macmillian: New York, 1982.

[8] Helgaker, T.; Jørgensen, P.; Olsen, J. *Molecular Electronic-Structure Theory;* John Wiley and Sons: New York, 2000.

[9] Levine, I. N. *Quantum Chemistry;* Pearson US Imports & PHIPEs: New York, 1998.

[10] Cramer, C. J. *Essentials of Computational Chemistry;* John Wiley and Sons Ltd: New York, 2004.

[11] Jensen, F. *Introduction to Computational Chemistry;* John Wiley and Sons Ltd: New York, 1998.

[12] Strange, P. *Relativistic Quantum Mechanics with Applications in Condensed Matter and Atomic Physics;* Cambridge Univ. Press: London, 1998 594 pp.

[13] Balasubramanian, K. *Relativistic Effects in Chemistry. Part A. Theory and Techniques;* Wiley: New York, 1997a 301 p.

[14] Oppenheimer, J. R.; Born, M. *Ann. Phys.* **1927,** *84,* 457.

[15] Hartree, D. R. *Proc. Cambridge Phil. Soc.* **1928,** *24(89),* 246.

[16] Pauli, W. *Z. Physik* **1925,** *31,* 765.

[17] Slater, J. C. *Phys. Rev.* **1929,** *34,* 1293.

[18] Slater, J. C. *Phys. Rev.* **1930,** *35,* 210.

[19] Fock, V. *Z. Physik* **1930,** *61,* 126.

[20] Møller, C.; Plesset, M. S. *Phys. Rev.* **1934,** *46,* 618.

[21] Olsen, J.; Roos, B. O.; Jørgensen, P.; Jensen, H. J. A. *J. Chem. Phys* **1988,** *89,* 2185.

[22] Olsen, J.; Christiansen, O.; Koch, H.; Jørgensen, P. *J. Chem. Phys.* **1996,** *105,* 5082.

[23] Olsen, J. *unpublished results* .

[24] Piecuch, P.; Kucharski, S. A.; Kowalski, K.; Musial, M. *Comput. Phys. Comm.* **2002,** *149,* 71.

[25] Bartlett, R. J. *Recent Advances in Coupled-Cluster Methods;* World Scientific Pub Co Inc: , 1997.

[26] Larsen, H.; Hald, K.; Olsen, J.; Jørgensen, P. *J. Chem. Phys.* **2001,** *115,* 3015.

[27] Lee, T. J.; Taylor, P. R. *Int. J. Quant. Chem.* **1989,** *S23,* 199.

[28] Schirmer, J.; Cederbaum, L. S.; Walter, O. *Phys. Rev. A* **1983,** *28,* 1237.

[29] Larsen, H.; Olsen, J.; Jørgensen, P.; Christiansen, O. *J. Chem. Phys.* **2000,** *113,* 6677.

[30] Harrison, R. J.; Handy, N. C. *Chem. Phys. Lett.* **1983,** *95,* 386.

[31] Langhoff, S. R.; Davidson, E. R. *Int. J. Quantum Chem.* **1974,** *8,* 61.

[32] Pople, J. A.; Head-Gordon, M.; Raghavachari, K. *J. Chem. Phys.* **1987,** *87,* 5968.

[33] Helgaker, T.; Ruden, T. A.; Jørgensen, P.; Olsen, J.; Klopper, W. *J. Phys. Org. Chem.* **2004,** *17,* 913.

[34] Roos, B. O.; Taylor, P. R.; Siegbahn, P. E. M. *Chem. Phys.* **1980,** *48,* 157.

[35] Andersson, K.; Malmqvist, P.-Å.; Roos, B. O. *J. Chem. Phys.* **1992,** *96,* 1218.

[36] Gagliardi, L.; Roos, B. O. *Nature* **2005,** *433,* 848.

[37] Hohenberg, P.; Kohn, W. *Phys. Rev.* **1964,** *B136,* 864.

[38] Dreizler, R. M.; Gross, E. K. U. *An Approach to the Quantum Many-Body Problem;* Springer-Verlag: Berlin, 1990.

[39] Levy, M. *Phys. Rev. A* **1982,** *26,* 1200.

[40] Kohn, W.; Sham, L. J. *Phys. Rev. A* **1965,** *140,* 1133.

[41] Vosko, S. J.; Wilk, L.; Nusair, M. *Can. J. Phys.* **1980,** *58,* 1200.

[42] Ma, S. K.; Brueckner, K. A. *Phys. Rev.* **1968,** *18,* 165.

[43] Stephens, P. J.; Devlin, F. J.; Chabalowski, C. F.; Frisch, M. J. *J. Phys. Chem.* **1994,** *98,* 11623.

[44] Perdew, J. A Primer in Density Functional Theory. In ; Springer-Verlag: Berlin, 2003; Chapter 1, page 1.

[45] Einstein, A. *Ann. Phys. Chem.* **1905,** *17,* 891.

[46] Klein, O. *Z. Physik* **1926,** *37,* 895.

[47] Gordon, W. *Z. Physik* **1926,** *40,* 117.

[48] Dirac, P. A. M. *Proc. R. Soc.* **1928,** *A117,* 610.

[49] Salpeter, E. E.; Bethe, H. A. *Phys. Rev.* **1951,** *84,* 1232.

[50] Breit, G. *Phys. Rev.* **1929,** *34,* 553.

[51] Visscher, L. *Theor. Chem. Acc.* **1997,** *98,* 68.

[52] Pedersen, J. K. *Description of Correlation and Relativistic Effects in Calculation of Molecular Properties,* Thesis, University of Odense, 2004.

[53] Belpassi, L.; Tarantelli, F.; Sgamellotti, A.; Quiney, H. M. *J. Chem. Phys.* **2006,** *124,* 124104.

[54] Dyall, K. G. *J. Chem. Phys.* **1994,** *100,* 2118.

[55] Saue, T.; Bakken, V.; Enevoldsen, T.; Helgaker, T.; Jensen, H. J. A.; Laerdahl, J. K.; Ruud, K.; Thyssen, J.; Visscher, L. "DIRAC, a relativistic ab initio electronic structure program, Release 3.2", http://dirac.chem.sdu.dk, 2000.

[56] Sundholm, D. Relativistic Electronic Structure Theory Part 1: Fundamentals. In ; Elsevier: Amsterdam, 2002; Chapter 13, page 758.

[57] Foldy, L.; Wouthuysen, S. *Phys. Rev.* **1950,** *78,* 29.

[58] Douglas, M.; Kroll, N. M. *Ann. Phys. (New York)* **1974,** *82,* 89.

[59] Hess, B. A. *Phys. Rev. A* **1986,** *33,* 3742.

[60] Hess, G. J. B. A. *Phys. Rev. A* **1989,** *39,* 6016.

[61] Brummelhuis, R.; Siedentop, H.; Stockmeyer, E. *Documenta Mathematica* **2002,** *7,* 167.

[62] "Amsterdam Density Functional program", Theoretical Chemistry, Vrije Universiteit, Amsterdam, 2002 URL: http://www.scm.com.

[63] Hellmann, H. G. A. *Quantenchemie;* Deuticke: Leipzig, 1937.

[64] Dolg, M.; Stoll, H.; Preuss, H. *Theor. Chim. Acta* **1993,** *85,* 441.

[65] Dolg, M. *to be published* .

[66] Lévy-Leblond, J.-M. *Comm. Math. Phys.* **1967,** *6,* 286.

[67] Saue, T. *Adv. Quantum Chem.* **2005,** *48,* 383.

[68] Desclaux, J. P. *Comput. Phys. Comm.* **1975,** *9,* 31.

[69] Laaksonen, L.; Pyykkö, P.; Sundholm, D. *Internat. J. Quantum Chem.* **1983,** *23,* 309.

[70] Marques, M. A. L.; Castro, A.; Bertsch, G. F.; Rubio, A. *Comput. Phys. Comm.* **2003,** *151,* 60.

[71] Roothaan, C. C. J. *Rev. Mod. Phys.* **1951,** *23,* 69.

[72] Hehre, W. J.; Stewart, R. F.; Pople, J. A. *J. Chem. Phys.* **1969,** *51,* 2657.

[73] Almlöf, J.; Taylor, P. R. *J. Chem. Phys.* **1987,** *86,* 4070.

[74] Karlström, G.; Lindh, R.; Malmqvist, P.-Å.; Roos, B. O.; Veryazov, U. R. V.; Widmark, P.-O.; Cossi, M.; Schimmelpfennig, B.; Neogrady, P.; Seijo, L. *Computational Material Science* **2003,** *28,* 222.

[75] Roos, B. O.; Lindh, R.; Malmqvist, P.-Å. *J. Phys. Chem. A* **2005,** *109,* 6575.

[76] Dunning, T. H. *J. Chem. Phys.* **1989,** *90,* 1007.

[77] Schäfer, A.; Horn, H.; Ahlrichs, R. *J. Chem. Phys.* **1992,** *97,* 2571.

[78] Ahlrichs, R.; Bär, M.; Häser, M.; Horn, H.; Kölmel, C. *Chem. Phys. Lett.* **1989,** *162,* 165.

[79] URL: http://www.emsl.pnl.gov/forms/basisform.html.

[80] Manninen, P.; Vaara, J. *J. Comput. Chem.* **2006,** *27,* 434.

[81] Saue, T.; Jensen, H. J. A. *J. Chem. Phys.* **2003,** *118,* 522.

[82] Hirshfeld, F. L. *Theor. Chim. Acta* **1977,** *44,* 129.

[83] te Velde, G. *Numerical integration and other methodological aspects of bandstructure calculations, in Chemistry,* Thesis, Vrije Universiteit Amsterdam, 1990.

[84] Becke, A. D.; Edgecombe, K. E. *J. Chem. Phys.* **1990,** *92,* 5397.

[85] Savin, A.; Nesper, R.; Wengert, S.; Fässler, T. F. *Angew. Chem. Int. Ed. Engl.* **1997,** *36,* 1808.

[86] Ziegler, T.; Rauk, A. *Inorg. Chem.* **1979,** *18,* 1558.

[87] Bickelhaupt, F. M.; Baerends, E. J. *Rev. Comp. Chem.* **2000,** *15,* 1.

[88] Buckingham, A. D.; Fowler, P. W.; Hutson, J. M. *Chem. Rev.* **1988,** *88,* 963.

[89] Boys, S. F.; Bernardi, F. *Mol. Phys.* **1970,** *18,* 553.

[90] Helgaker, T. *et al.* "DALTON, a molecular electronic structure program, Release 1.2", 2001.

[91] Schmidt, M. W.; Baldridge, K. K.; Boatz, J. A.; Elbert, S. T.; Gordon, M. S.; Jensen, J. H.; Koseki, S.; Matsunaga, N.; Nguyen, K. A.; Su, S. J.; Windus, T. L.; Dupuis, M.; Montgomery, J. A. *J. Comput. Chem.* **1993,** *14,* 1347.

[92] Frisch, M. J. *et al.* "Gaussian 03, Revision C.02", Gaussian, Inc., Wallingford, CT, 2004.

[93] Kohout, M. "Program 'Dgrid'", Max-Planck-Institut für Chemische Physik fester Stoffe, Dresden, 2001.

[94] URL: http://www.csc.fi/gopenmol/index.phtml.

[95] Hassinen, T.; Peräkylä, M. *J. Comput. Chem.* **2001,** *22,* 1229.

[96] Schaftenaar, G.; Noordik, J. H. *J. Computer-Aided Mol. Design* **2000,** *14,* 123.

[97] Portmann, S.; Lüthi, H. P. *CHIMIA* **2000,** *54,* 766.

[98] URL: http://www.nongnu.org/xmakemol/.

[99] Kaupp, M.; von Schnering, H. G. *Angew. Chem., Int. Ed.* **1993,** *32,* 861.

[100] Riedel, S.; Straka, M.; Kaupp, M. *Chem. Eur. J.* **2005,** *11,* 2743.

[101] Fischer, R. A.; Weiss, J. *Angew. Chem. Int. Ed.* **1999,** *38,* 2830.

[102] Linti, G.; Schnöckel, H. *Coord. Chem. Rev.* **2000,** *206,* 285.

[103] Irvine, G. J.; Lesley, M. J. G.; Marder, T. B.; Norman, N. C.; Rice, C. R.; Robins, E. G.; Roper, W. R.; Whittell, G. R.; Wright, L. J. *Chem. Rev.* **1998,** *98,* 2685.

[104] Braunschweig, H. *Angew. Chem. Int. Ed.* **1998,** *37,* 1786.

[105] Wrackmeyer, B. *Angew. Chem. Int. Ed.* **1999,** *38,* 771.

[106] Robinson, G. H. *Organometallics* **1997,** *16,* 4511.

[107] Cotton, F. A.; Feng, X. J. *Organometallics* **1998,** *17,* 128.

[108] Frenking, G.; Boehme, C. *Chem. Eur. J.* **1999,** *5,* 2184.

[109] Uddin, J.; Boehme, C.; Frenking, G. *Organometallics* **1999,** *19,* 571.

[110] Uddin, J.; Frenking, G. *J. Am. Chem. Soc.* **2001,** *123,* 1683.

[111] Frenking, G. *J. Organomet. Chem.* **2001,** *635,* 9.

[112] Doerr, M.; Frenking, G. *Z. Anorg. Allg. Chem.* **2002,** *628,* 843.

[113] Frenking, G.; Wichmann, K.; Fröhlich, N.; Grobe, J.; Golla, W.; Van, D. L.; Krebs, B.; Läge, M. *Organometallics* **2002,** *21,* 2921.

[114] Uhl, W.; Pohlmann, M.; Wartchow, R. *Angew. Chem. Int. Ed.* **1998,** *37,* 961.

[115] Uhl, W.; Melle, S. *Z. Anorg. Allg. Chem.* **2000,** *626,* 2043.

[116] Jalilehvand, F.; Maliarik, M.; Sandström, M.; Mink, J.; Persson, I.; Persson, P.; Tóth, I.; Glaser, J. *Inorg.Chem.* **2001,** *40,* 3889.

[117] Jalilehvand, F.; Ericson, F.; Glaser, J.; Maliarik, M.; Mink, J.; Sandström, M.; Tóth, I.; Tóth, J. *Chem. Eur. J.* **2001,** *7,* 2167.

[118] Maliarik, M.; Glaser, J.; Tóth, I. *Inorg. Chem.* **1998,** *37,* 5452.

[119] Maliarik, M.; Berg, K.; Glaser, J.; Sandström, M.; Tóth, I. *Inorg. Chem.* **1998,** *37,* 2910.

[120] Maliarik, M.; Glaser, J.; Tóth, I.; da Silva, M. W.; Zekany, L. *Eur. J. Inorg. Chem.* **1998,** *1998,* 565.

[121] Ma, G.; Fischer, A.; Glaser, J. *Eur. J. Inorg. Chem.* **2002,** *2002,* 1307.

[122] Dolg, M.; Pyykkö, P.; Runeberg, N. *Inorg. Chem.* **1996,** *35,* 7450.

[123] Autschbach, J.; Ziegler, T. *J. Am. Chem. Soc.* **2001,** *123,* 5320.

[124] Russo, M. R.; Kaltsoyannis, N. *Inorg. Chim. Acta* **2001,** *312,* 221.

[125] Pyykkö, P.; Patzschke, M. *Faraday Discussions* **2003,** *124,* 41.

[126] Pyykkö, P. *Chem. Rev.* **1997,** *97,* 597.

[127] Bollwein, T.; Brothers, P. J.; Hermann, H. L.; Schwerdtfeger, P. *Organometallics* **2002,** *21,* 5236.

[128] Crawford, M. J.; Mayer, P.; Noth, H. *Inorg. Chem.* **2004,** *43,* 6860.

[129] Pyykkö, P.; Desclaux, J. P. *Acc. Chem. Res.* **1979,** *12,* 276.

[130] Barysz, M.; Pyykkö, P. *Chem. Phys. Lett.* **1998,** *285,* 398.

[131] Gibson, J. K. *J. Vac. Sci. Technol. A* **1998,** *16,* 653.

[132] Pyykkö, P.; Runeberg, N. *Angew. Chem., Int. Ed.* **2002,** *41,* 2174.

[133] Li, X.; Kiran, B.; Li, J.; Zhai, H.-J.; Wang, L.-S. *Angew. Chem., Int. Ed.* **2002,** *41,* 4786.

[134] Schroeder, H.; Stritzker, B. *Radiation Effects* **1977,** *33,* 125.

[135] Knecht, J.; Fischer, R.; Overhof, H.; Hensel, F. *J. Chem. Soc., Chem. Comm.* **1978,** 905.

[136] Schmidbaur, H.; Hamel, A.; Mitzel, N. W.; Schier, A.; Nogai, S. *Proc. Natl. Acad. Sci. USA* **2002,** *99,* 4919.

[137] Schneider, D.; Nogai, S.; Schier, A.; Schmidbaur, H. *Inorg. Chim. Acta* **2003,** *179,* 352.

[138] Polak, M.; Gruebele, M.; Saykally, R. J. *J. Chem. Phys.* **1987,** *87,* 3352.

[139] Pyykkö, P.; Runeberg, N.; Mendizabal, F. *Chem. Eur. J.* **1997,** *3,* 1451.

[140] Klamt, A.; Schüürmann, G. *J. Chem. Soc., Perkin Trans.* **1993,** *II,* 799.

[141] Schädel, M. *The Chemistry of Superheavy Elements;* Kluwer Academic Publishers: Dordrecht, 2003.

[142] Smolanczuk, R. *Acta Phys. Pol. B* **1999,** *30,* 1565.

[143] Waber, J. T.; Cromer, D. T.; Liberman, D. *J. Chem. Phys.* **1969,** *51,* 664.

[144] Seth, M.; Cooke, F.; Schwerdtfeger, P.; Heully, J.-L.; Pelissier, M. *J. Chem. Phys.* **1998,** *109,* 3935.

[145] Pyykkö, P.; Riedel, S.; Patzschke, M. *Chem. Eur. J.* **2005,** *11,* 3511.

[146] Gagliardi, L.; Pyykkö, P. *Angew. Chem. Int. Ed.* **2004,** *43,* 1573.